Universidade Federal do Rio Grande do Norte

Centro de Ciências Exatas e da Terra

Programa de Pós-Graduação em Física

An Effective Model for Strongly Correlated Electrons

Hernán Guillermo Bueno Xavier

Natal-RN

Fevereiro de 2019

Hernán Guillermo Bueno Xavier

An Effective Model for Strongly Correlated Electrons

Dissertação apresentada ao Programa de Pós-Graduação em Física da Universidade Federal do Rio Grande do Norte como requisito parcial para obtenção do grau de Mestre em Física.

Advisor:
Prof. Dr. Álvaro Ferraz Filho

Universidade Federal do Rio Grande do Norte - UFRN
Programa de Pós-Graduação em Física - PPGF

Natal-RN
Fevereiro de 2019

Universidade Federal do Rio Grande do Norte - UFRN
Sistema de Bibliotecas - SISBI
Catalogação de Publicação na Fonte. UFRN - Biblioteca Central Zila Mamede

Xavier, Hernán Guillermo Bueno.
An Effective Model for Strongly Correlated Electrons / Hernán Guillermo Bueno Xavier. - 2019.
74 f.: il.

Dissertação (mestrado) - Universidade Federal do Rio Grande do Norte, Centro de Ciências Exatas e da Terra, Programa de Pós-Graduação em Física, Natal, RN, 2019.
Orientador: Prof. Dr. Álvaro Ferraz Filho.

1. Física - Dissertação. 2. Cupratos de alta-Tc - Dissertação. 3. Modelo t-J - Dissertação. 4. Elétrons fortemente correlacionados - Dissertação. 5. Teoria de campos efetiva - Dissertação. I. Ferraz Filho, Álvaro. II. Título.

RN/UF/BCZM CDU 53

Elaborado por Ana Cristina Cavalcanti Tinôco - CRB-15/262

Abstract

In this work we examine an alternative effective formulation for the t-J model which is believed to capture the essential physics behind the underdoped regime of the high-T_c cuprates. After recasting the original problem into this representation, we check the consistency of the procedure and discuss some physical consequences of such a representation, including, the crossover between the regimes of small and large Fermi surfaces which is observed experimentally. We then explore the possiblity of constructing a path integral representation of the partition function of the the t-J model by departing from the formulation presented. Finally, we use the latter formalism to derive a continuum effective field theory in $(2+1)$ spacetime dimensions which features small hole-like pockets near the nodal regions of the Brillouin zone along with an unconventional mechanism for superconductivity.

Keywords: strongly correlated electrons; t-J model; high-T_c cuprates; effective field theory.

Resumo

Neste trabalho examinamos uma formulação efetiva para o modelo t-J, o qual se acredita capturar a física por trás do regime de baixa dopagem dos cupratos de alta-T_c. Depois de reformular o problema original nesta representação, verificamos a consistência do procedimento e discutimos algumas consequências físicas dessa representação, incluindo, a transição entre os regimes de pequena e grande superfícies de Fermi que observada experimentalmente. Em seguida, exploramos a possibilidade de construir uma representação por integrais de caminho para a função de partição do modelo t-J partindo da formulação apresentada. Finalmente, fazendo uso desse formalismo derivamos uma teoria de campos contínua em $(2+1)$ dimensões de espaço-tempo que exibe pequenos *pockets* do tipo buraco próximos às regiões nodais da zona de Brillouin em conjunto com um mecanismo não convencional para supercondutividade.

Palavras-chave: elétrons fortemente correlacionados; modelo t-J, cupratos de alta-T_c; teoria de campos efetiva.

Acknowledgements

I am grateful to my advisor professor Álvaro Ferraz for his trust and dedication to offer a solid academic background to my training. I thank the whole staff of DFTE and IIP, especially the professors who contributed into my instruction as well. I also thank the friends and colleagues who make the UFRN physics community a pleasant academic environment. The present work was also made possible by the care of my family, especially my parents Regina and Hugo, and the emotional support from Theresa. This study was financed in part by the Coordenação de Aperfeiçoamento de Pessoal de Nível Superior - Brasil (CAPES) - Finance Code 001.

List of Figures

Contents

Chapter 1

Introduction

Despite the long time since its discovery in 1986 [1], the high-temperature superconductors are still a challenge to the condensed matter physics community which struggle to figure out the physical properties of such strongly correlated electronic system. In this chapter, we will introduce the reader to the subject by first presenting some basic features of the hole doped phase diagram of the so called cuprates family. Then, after this piece of experimental information, we will shortly discuss the Hubbard and t-J models which are believed to describe the physics of such compounds. Soon after that, we end this chapter by commenting on the organizational structure of this dissertation.

1.1 Phase Diagram of the Hole Doped Cuprates

Although there are lots of different high-temperature superconducting cuprates, they all are layered materials made up of copper-oxide planes separated by several elements, such as La in the $La_{2-x}Sr_xCuO_4$ (LSCO), whose chemistry controls the density of dopant carriers $\delta(x)$ in the CuO_2 layers.[1] They also share a very similar phase diagram largely shaped by competing phases whose physical nature are still controversial [2].

Let us start from the undoped system ($x = 0$). In this scenario there is just one electron per Cu site which accordingly to the standard band theory would give rise to a single half-filled band. Consequently, the system should be metallic. However, due to the existence of strong electron-electron interactions, this simple independent electron picture

[1] The precise functional relation between the density of vacancies $\delta(x)$ and the stoichiometric parameter x will depend on the specificities of each compound, e.g., the number of planes per unit cell. Later in the text, we shall only concentrate on δ since it is a much simpler theoretical parameter to deal with.

breaks down and the system is turned instead into an insulating antiferromagnetic (AF) phase. Because of this, such a class of materials are often denominated Mott insulators in order to differentiate them from the regular band insulators.

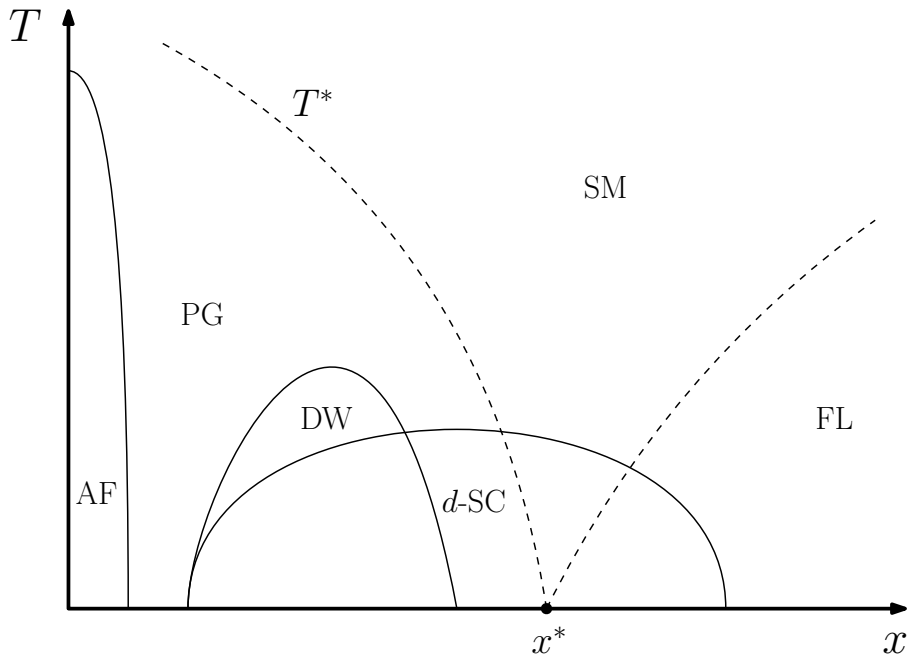

Figure 1.1: Schematic phase diagram for temperature T versus doping x of the hole-doped high-T_c cuprate superconductors.

Upon hole doping the compound, the long range AF order is rapidily destroyed (tipically after $\delta \sim 0.03$), as we can see from the narrow AF region in the schematic phase diagram given at the Figure 1.1. For temperatures below $T^*(x)$, in its place emerges the puzzling pseudogap (PG) phase. The PG is frequently related to a depletion of the accessible states near the anti-nodal regions $(\pm\pi, 0)$ and $(0, \pm\pi)$ of the Brillouin zone (BZ). This fact can be detected most directly by angle-resolved photoemission spectroscopy (ARPES) experiments [3]. In the panels (a) and (b) of Figure 1.2, we reproduce some photoemission results of Shen et al. [4] for $Ca_{2-x}Na_xCuO_2Cl_2$ (Na-CCOC) at $x = 0.05$ and $x = 0.10$, respectively. Their findings reveal that most of the spectral intensity is concentrated in a small region near the nodal position $(\frac{\pi}{2}, \frac{\pi}{2})$ within the first quadrant of the BZ.

By further doping, the cuprates eventually undergo into its most illustrious phase, the d-wave superconducting (d-SC) phase. This phase transition is characterized by a critical temperature $T_c(x)$ which starts at zero for some lower bound critical doping, increases up to the optimal doping and finally decays to zero, thereby forming a superconducting

dome in the T versus x phase diagram, like the one presented in Figure 1.1. Around optimal doping, the T_c of the cuprates is much larger than what one could expect for a superconductor described by a conventional Bardeen-Cooper-Schrieffer (BCS) theory. The designation d-wave for the SC phase of the cuprates comes directly from experiments indicating a $d_{x^2-y^2}$ pairing symmetry on the system, see for example [5]. This implies that its order parameter transforms like an $l = 2$ angular momentum state under the action of the rotation group.[2]

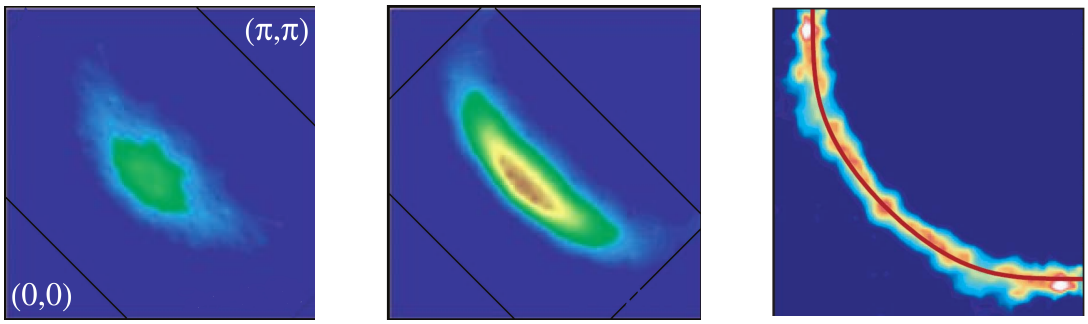

(a) (b) (c)

Figure 1.2: Distribution of ARPES spectral function in the first quadrant of the BZ for different doping levels in cuprates. In parts (a) and (b), results for underdoped samples of Na-CCOC from [4]. In part (c), results for an overdoped sample of Tl2201 from [6].

Still in the underdoped regime (around $x = 1/8$), there is also an incommensurate bidirectional charge density wave (DW) order detected through x-ray diffraction and scanning tunneling microscopy experiments. There is strong evidence that the DW modulation vectors lie in the copper-oxide planes and they take the form $(\pm Q_0, 0)$ and $(0, \pm Q_0)$ with a decreasing Q_0 for a increasing hole doping [7]. The wavelength periods range from 3 to 5 lattice spacings. The measurements also point to a predominantly d-wave form factor to its order parameter. For temperatures below $T_c(x)$, it seems likely that the SC and DW phases compete with each other [8].

This underdoped portion of the phase diagram that we have been discussing so far is also associated to a system with a small Fermi surface (FS), as supported by quantum oscillations experiments [9]. More recently, performing Hall coefficient measurements in cuprates, Badoux et al. [10] detected a change on the in-plane carrier density n from $n = \delta$ (underdoped) to $n = 1 + \delta$ (overdoped) happening across the PG critical point x^*.

Right above the d-SC dome, for some range of doping, one finds an anomalous metallic

[2]Just to put it simply, it means that the SC order parameter changes sign under a $\frac{\pi}{2}$-rotation.

phase known as the strange metal (SM) phase. This phase is anomalous in the sense that it features a non-Fermi liquid behavior. For instance, the in-plane resistivity ρ on the SM phase has a linear behavior with respect to the temperature, $\rho \propto T$. Unfortunately, the present understanding of this phase seems to be even more rudimentary than the one about the PG [2].

Finally, at the heavily overdoped regime the system becomes a conventional Fermi liquid (FL) with a large hole-like FS as revealed by ARPES studies. In panel (c) of Figure 1.2, we reproduce the results obtained by Platé et al. [6] for an overdoped sample of $Tl_2Ba_2CuO_{6+x}$ (Tl2201). There, we can observe the existence of a continuous cylindrical FS centered at (π, π) which matches the Luttinger volume corresponding to a $n = 1 + \delta$ carrier density FL with $\delta = 0.25$.

1.2 From Hubbard to the t-J Model

Soon after the discovery of the high-T_c superconductors, Anderson [11] suggested that the correct model to describe the copper-oxide planes in such materials is the two-dimensional Hubbard model without phonons. In second quantized language this one-band Hamiltonian can be written as

$$H = -\sum_{ij\sigma} \left(t_{ij} c^{\dagger}_{i\sigma} c_{j\sigma} + \text{h.c.} \right) + U \sum_{i} n_{i\uparrow} n_{i\downarrow}, \tag{1.1}$$

where the operator $c^{\dagger}_{\sigma}$ (c_{σ}) creates (annihilates) an electron at the lattice site i with spin polarization σ, and $n_{i\sigma} = c^{\dagger}_{\sigma} c_{\sigma}$ is the number operator. Indeed, the physical meaning behind the Hamiltonian (1.1) can be easily understood. While the second term describes an on-site Coulomb repulsion with strength $U > 0$, the tunneling processes between the atomic orbitals localized on individual lattice sites are described by the first term through the hopping amplitudes t_{ij}.

As commented above, it turns out that in the cuprates the electron-electron repulsion U is large compared to the kinetic energy scale $|t|$. By considering the limit $|t| \ll U$ of equation (1.1), the doubly occupied states become inhibited and one will end up with the so called t-J model. This latter model is represented in terms of the following projected

Hamiltonian

$$H_{t\text{-}J} = -\sum_{ij\sigma} \left(t_{ij} \tilde{c}^{\dagger}_{i\sigma} \tilde{c}_{j\sigma} + \text{h.c.} \right) + \sum_{ij} J_{ij} \left(\boldsymbol{Q}_i \cdot \boldsymbol{Q}_j - \tfrac{1}{4} \tilde{n}_i \tilde{n}_j \right), \tag{1.2}$$

where $\tilde{c}_{i\sigma} = c_{i\sigma}(1 - n_{i\bar{\sigma}})$ is the Gutzwiller projected electron operator, $\tilde{n}_i = \tilde{c}^{\dagger}_i \tilde{c}_i = n_{i\uparrow} + n_{i\downarrow} - 2n_{i\uparrow}n_{i\downarrow}$ is the projected occupation number, $\boldsymbol{Q}_i = \frac{1}{2} \tilde{c}^{\dagger}_i \boldsymbol{\sigma} \tilde{c}_i$ is the electron spin operator and $\boldsymbol{\sigma}$ are the Pauli matrices.[3] The exchange couplings $J_{ij} \sim \mathcal{O}(t^2/U)$ appearing in the Hamiltonian arise from second-order virtual processes containing doubly occupied states, as is depicted schematically in Figure 1.3. From this construction, it should be clear that the on-site Hilbert space of the t-J model at any site i is just made up by the states

$$\mathcal{H}^{t\text{-}J}_i = \left\{ \left|0\right\rangle_i, \left|\uparrow\right\rangle_i, \left|\downarrow\right\rangle_i \right\}, \tag{1.3}$$

with the on-site doubly occupied electron state $\left|\uparrow\downarrow\right\rangle_i$ being now strictly forbidden.

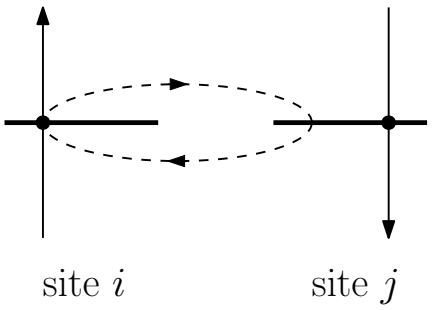

Figure 1.3: Example of a virtual two-step hopping process responsible for the appearance of the exchange coupling.

Precisely at half-filling, the t-J Hamiltonian reduces to the Heisenberg AF model

$$H_{\text{AF}} = J \sum_{\langle ij \rangle} \boldsymbol{Q}_i \cdot \boldsymbol{Q}_j, \tag{1.4}$$

where we have restricted the exchange couplings to nearest neighbor interactions for simplicity here. For bipartite lattices $L = A \oplus B$ (i.e. lattices in which the first neighbors of one sublattice belong to the other sublattice), the exact quantum ground-state is close to the AF Néel state where the neighboring spins are aligned antiparallel to each other. Including quantum fluctuations on top of this reference state leads to spin-wave excitations which are indeed observed experimentally on cuprates [12].

[3] We have adopted the shorthand notation $\tilde{c}_i = \begin{pmatrix} \tilde{c}_{i\uparrow} & \tilde{c}_{i\downarrow} \end{pmatrix}^T$ for the projected electron spinor operator.

1.3 About the Structure of this Work

After this short exposition of the experimental and theoretical backgrounds of high-T_c cuprates, we are ready to move into the core aspects of the present work which are structured as follows.

In Chapter 2, we review the so called doped carrier formulation with the objective to address doped spin systems through a different starting point. As a matter of fact, after adding a necessary constraint into the formalism, we then introduce an effective formulation for the canonical t-J model.

In Chapter 3, we first verify the faithfulness of such Hamiltonian formulation by the solution of two simple problems. After completing this task, we comment on some physical consequences associated with such a description for the cuprates.

In Chapter 4, we explore the possiblity of writing a functional field integral for the quantum partition function of the problem. From that we derive an effective field theory especially suited for a lightly doped scenario.

Finally, in Chapter 5, we draw some conclusions for this work and indicate open perspectives which should be object of future research.

On the course of preparation of this work, the author has consulted diverse textbooks from where most of our adopted conventions were borrowed, such as the use of a convenient set of units $\hbar = c = k_B = 1$. These references shall also provide extra information in some topics and can be consulted freely by the reader, if needed. In the subject of condensed matter field theory and many-body physics, Altland and Simons [13], Fradkin [14], and Marino [15]. For quantum field theory methods, Peskin and Schroeder [16], and Polyakov [17].

Chapter 2

The Doped Carrier Formulation

Since it will be our adopted language in the rest of the work, we are going to dedicate the most part of this chapter to briefly review an alternative representation of the doped t-J model proposed by Ribeiro and Wen [18, 19] known as the doped carrier formulation. Then, by using their formulation as a starting point, we are going to present an effective Hamiltonian description of the t-J model which lives on an unrestricted Hilbert space.

2.1 The Enlarged Hilbert Space

The doped carrier formulation consists on replacing the original projected electron operators by an arrangement of spin-$\frac{1}{2}$ localized objects and dopant spin-$\frac{1}{2}$ fermions known as lattice spins and dopons respectively. By doing this, one needs to enlarge the on-site Hilbert space at each lattice site i in order to accomodate those new degrees of freedom. This enlarged space is then spanned by the states

$$|\sigma a\rangle_i \equiv |\sigma\rangle_i \otimes |a\rangle_i \,, \tag{2.1}$$

where $\sigma = \{\Uparrow, \Downarrow\}$ represents the projection of the lattice spin and $a = \{0, \uparrow, \downarrow\}$ are the dopon states (here once again the doubly occupied states are forbidden). Thereby, the enlarged on-site Hilbert space at any site i will explicitly be

$$\mathcal{H}_i^{\text{enl}} = \left\{ |\Uparrow 0\rangle_i \,, |\Downarrow 0\rangle_i \,, |\Uparrow\uparrow\rangle_i \,, |\Downarrow\uparrow\rangle_i \,, |\Uparrow\downarrow\rangle_i \,, |\Downarrow\downarrow\rangle_i \right\}. \tag{2.2}$$

To act on these states we introduce the lattice spin operator $\boldsymbol{S}_i \in su(2)$ and the fermionic Gutzwiller projected annihilation dopon operator $\tilde{d}_{i\sigma} = d_{i\sigma}(1 - d^\dagger_{i\bar{\sigma}} d_{i\bar{\sigma}}) \equiv d_{i\sigma}(1 - n^d_{i\bar{\sigma}})$, since we are working on a Hilbert space without doubly occupied dopon states.

Then, to make contact with physical operators one must define a suitable mapping between the states of the two on-site Hilbert spaces (1.3) and (2.2). For instance, this can be accomplished by identifying the states with the same total spin and spin projection quantum numbers on both formulations, i.e.,

$$|0\rangle_i \;\leftrightarrow\; \frac{|\Uparrow\downarrow\rangle_i - |\Downarrow\uparrow\rangle_i}{\sqrt{2}}\,, \quad |\uparrow\rangle_i \;\leftrightarrow\; |\Uparrow 0\rangle_i \quad \text{and} \quad |\downarrow\rangle_i \;\leftrightarrow\; |\Downarrow 0\rangle_i\,. \tag{2.3}$$

Thus, within this picture, a vacancy in the electronic system corresponds to a singlet made up of a lattice spin and a dopon whereas the presence of an electron is related to the absence of the dopon. The remaining triplet states

$$\frac{|\Uparrow\downarrow\rangle_i + |\Downarrow\uparrow\rangle_i}{\sqrt{2}}\,, \quad |\Uparrow\uparrow\rangle_i \quad \text{and} \quad |\Downarrow\downarrow\rangle_i\,, \tag{2.4}$$

on the other hand, belong to the unphysical subspace of $\mathcal{H}_i^{\text{enl}}$ and must be eliminated in practical calculations.

2.2 The Electron Operator in the Spin-Dopon Representation

Given the map rules above we can construct an operator whose action on the on-site enlarged Hilbert space matches the operational properties of the original projected electron operator $\tilde{c}^\dagger_{i\sigma}$. In other words, when written in terms of the spin-dopon variables this operator must satisfy[1]

$$\tilde{c}^\dagger_{i\sigma} \frac{|\Uparrow\downarrow\rangle_i - |\Downarrow\uparrow\rangle_i}{\sqrt{2}} = |\sigma 0\rangle_i \qquad \text{and} \qquad \tilde{c}^\dagger_{i\sigma}\,|\Uparrow 0\rangle_i = \tilde{c}^\dagger_{i\sigma}\,|\Downarrow 0\rangle_i = 0. \tag{2.5}$$

Further requiring that the operator representation of $\tilde{c}^\dagger_{i\sigma}$ vanishes upon acting on the unphysical states, we also need to satisfy

$$\tilde{c}^\dagger_{i\sigma} \frac{|\Uparrow\downarrow\rangle_i + |\Downarrow\uparrow\rangle_i}{\sqrt{2}} = \tilde{c}^\dagger_{i\sigma}\,|\Uparrow\uparrow\rangle_i = \tilde{c}^\dagger_{i\sigma}\,|\Downarrow\downarrow\rangle_i = 0. \tag{2.6}$$

[1]Be careful with our abuse of notation here. The operator $\tilde{c}^\dagger_{i\sigma}$ in these equations is a function of the spin-dopon variables which mimetizes the properties of the electron operator within $\mathcal{H}_i^{\text{enl}}$.

To earn some confidence with the formalism, and to help us on the identification of the electron operator, let us inspect the action of some spin-dopon operators on the physical states. To begin with, consider $\tilde{d}_{i\sigma}$. It gives us that

$$\tilde{d}_{i\downarrow}\frac{|\Uparrow\downarrow\rangle_i - |\Downarrow\uparrow\rangle_i}{\sqrt{2}} = \frac{1}{\sqrt{2}}\,|\Uparrow 0\rangle_i \ , \qquad \tilde{d}_{i\uparrow}\frac{|\Uparrow\downarrow\rangle_i - |\Downarrow\uparrow\rangle_i}{\sqrt{2}} = -\frac{1}{\sqrt{2}}\,|\Downarrow 0\rangle_i$$

$$\text{and} \qquad \tilde{d}_{i\sigma}\,|\Uparrow 0\rangle_i = \tilde{d}_{i\sigma}\,|\Downarrow 0\rangle_i = 0. \tag{2.7}$$

Then, by comparing with (2.5), one can get the operator identity

$$\tilde{c}^{\dagger}_{i\sigma} = \mathrm{sgn}(\sigma)\sqrt{2}\mathcal{P}_i\tilde{d}_{i\bar{\sigma}}\mathcal{P}_i, \tag{2.8}$$

where $\mathrm{sgn}(\sigma = \uparrow,\downarrow) = \pm 1$ with $\bar{\sigma} = -\sigma$, and $\mathcal{P}_i$ is an on-site projection operator whose action projects states from $\mathcal{H}_i^{\mathrm{enl}}$ onto the physical subspace $\mathcal{H}_i^{\mathrm{phys}} \subset \mathcal{H}_i^{\mathrm{enl}}$ [20]. In a similar manner we also verify the action of the operator $S_i^{\sigma}\tilde{d}_{i\sigma}$, namely,

$$S_i^{-}\tilde{d}_{i\downarrow}\frac{|\Uparrow\downarrow\rangle_i - |\Downarrow\uparrow\rangle_i}{\sqrt{2}} = \frac{1}{\sqrt{2}}\,|\Downarrow 0\rangle_i \ , \qquad S_i^{+}\tilde{d}_{i\uparrow}\frac{|\Uparrow\downarrow\rangle_i - |\Downarrow\uparrow\rangle_i}{\sqrt{2}} = -\frac{1}{\sqrt{2}}\,|\Uparrow 0\rangle_i$$

$$\text{and} \qquad S_i^{\sigma}\tilde{d}_{i\sigma}\,|\Uparrow 0\rangle_i = S_i^{\sigma}\tilde{d}_{i\sigma}\,|\Downarrow 0\rangle_i = 0. \tag{2.9}$$

From this we now get that

$$\tilde{c}^{\dagger}_{i\sigma} = -\mathrm{sgn}(\sigma)\sqrt{2}\mathcal{P}_i S_i^{\sigma}\tilde{d}_{i\sigma}\mathcal{P}_i. \tag{2.10}$$

Combining the results above, one is able to recognize that the projected electron operator can be written as

$$\tilde{c}^{\dagger}_{i\sigma} \equiv \frac{\mathrm{sgn}(\sigma)}{\sqrt{2}}\Big[\left(\tfrac{1}{2} + \mathrm{sgn}(\sigma)S_i^z\right)\tilde{d}_{i\bar{\sigma}} - S_i^{\sigma}\tilde{d}_{i\sigma}\Big] \tag{2.11}$$

within the enlarged Hilbert space [19]. An advantage of this operator representation for $\tilde{c}^{\dagger}_{i\sigma}$ is that it indeed fulfills the defining relations on (2.5) and (2.6) without the need of any aid from the on-site projection operators.

2.3 The t-J Hamiltonian in the Spin-Dopon Formulation

Now we are in position to translate the projected electron t-J Hamiltonian (1.2) in terms of the lattice spin and projected dopon operators. Before moving forward though, let us shortly comment on a subtlety in the procedure of finding a faithful representation for $H_{t\text{-}J}$. To make our point clear, notice that we can generally write this Hamiltonian as

$$H_{t\text{-}J} = \mathcal{P} H^{\text{enl}} \mathcal{P}, \tag{2.12}$$

where $\mathcal{P} = \prod_i \mathcal{P}_i$ is a global projection operator and H^{enl} is a Hamiltonian defined in the enlarged Hilbert space $\mathcal{H}^{\text{enl}} = \prod_i \mathcal{H}_i^{\text{enl}}$. This tell us is that different choices of H^{enl} can still lead to the same t-J model after being projected [20]. Because of this ambiguity, let us pick a "gauge" for H^{enl} which turns our forthcoming analisys easier. We then choose a representation of H^{enl} in which the only nonvanishing matrix elements are those related to physical processes.

Let us start by rewriting the hopping term,

$$H_t = -\sum_{ij\sigma} \left(t_{ij} \tilde{c}^\dagger_{i\sigma} \tilde{c}_{j\sigma} + \text{h.c.} \right). \tag{2.13}$$

By replacing the operator identity (2.11) for $\tilde{c}^\dagger_{i\sigma}$ in the expression for H_t, we get the following representation of the hopping term in the enlarged Hilbert space,

$$\begin{aligned} H_t^{\text{enl}} &= \sum_{ij} \frac{t_{ij}}{2} \begin{pmatrix} \tilde{d}^\dagger_{j\uparrow} & \tilde{d}^\dagger_{j\downarrow} \end{pmatrix} \begin{pmatrix} \frac{1}{2} - S^z_j & -S^-_j \\ -S^+_j & \frac{1}{2} + S^z_j \end{pmatrix} \begin{pmatrix} \frac{1}{2} - S^z_i & -S^-_i \\ -S^+_i & \frac{1}{2} + S^z_i \end{pmatrix} \begin{pmatrix} \tilde{d}_{i\uparrow} \\ \tilde{d}_{i\downarrow} \end{pmatrix} + \text{h.c.} \\ &\equiv \sum_{ij} \frac{t_{ij}}{2} \left[\tilde{d}^\dagger_i \left(\tfrac{1}{2} - \boldsymbol{\sigma} \cdot \boldsymbol{S}_i \right) \left(\tfrac{1}{2} - \boldsymbol{\sigma} \cdot \boldsymbol{S}_j \right) \tilde{d}_j + \text{h.c.} \right] \end{aligned} \tag{2.14}$$

provided that $t_{ij} = t_{ji}$. To ease the notation in the formula above, we have introduced the two component spinor $\tilde{d}_i = \begin{pmatrix} \tilde{d}_{i\uparrow} & \tilde{d}_{i\downarrow} \end{pmatrix}^T$. From its construction, we can easily see that the action of H_t^{enl} corresponds to a hopping process of the form

$$\frac{|\Uparrow\downarrow\rangle_i - |\Downarrow\uparrow\rangle_i}{\sqrt{2}} \otimes |\sigma 0\rangle_j \;\rightarrow\; |\sigma 0\rangle_i \otimes \frac{|\Uparrow\downarrow\rangle_j - |\Downarrow\uparrow\rangle_j}{\sqrt{2}} \tag{2.15}$$

leaving the remaining sites unaltered. In view of (2.3), a process like the one above is

equivalent to

$$|0\rangle_i \otimes |\sigma\rangle_j \;\rightarrow\; |\sigma\rangle_i \otimes |0\rangle_j \,, \tag{2.16}$$

in the original projected electron picture, as one should expect. Furthermore, since the operator representation of $\tilde{c}^{\dagger}_{i\sigma}$ on equation (2.11) also satisfies the condition (2.6), H_t^{enl} will vanish upon action on sites containing (unphysical) triplet states. In other words, this means that only local singlet states hop between different lattice sites whereas the triplet states are localized and have no kinetic energy [19].

Notice that we could have used the identity in (2.8) to arrive at a seemingly simpler version of the hopping term,

$$H_t^{\text{enl}} = \sum_{ij\sigma} 2\big(t_{ij}\tilde{d}^{\dagger}_{i\sigma}\tilde{d}_{j\sigma} + \text{h.c.}\big). \tag{2.17}$$

Undoubtedly, this representation is as good as the one presented before and shall lead to the same physical conclusions if used properly. However, since it does not explicitly vanishes when acting on unphysical states its use may prove to be more involved in some cases.

We then move to the magnetic interaction term

$$H_J = \sum_{ij} J_{ij}\left(\boldsymbol{Q}_i \cdot \boldsymbol{Q}_j - \tfrac{1}{4}\tilde{n}_i\tilde{n}_j\right). \tag{2.18}$$

However this time we use a different strategy than a simply substitution of the projected electron operator identity. Consider first the total on-site spin operator $\boldsymbol{J}_i = \boldsymbol{S}_i + \boldsymbol{S}_i^d$, where $\boldsymbol{S}_i^d = \frac{1}{2}\tilde{d}_i^{\dagger}\boldsymbol{\sigma}\tilde{d}_i$ denotes the dopon spin operator. From the previous discussion on the on-site spin equivalence, it should be clear that the physical electron spin should read $\boldsymbol{Q}_i = \mathcal{P}_i\boldsymbol{J}_i\mathcal{P}_i$. Nonetheless, as one can readily verify, an equivalent and more handy relation is

$$\boldsymbol{Q}_i = \mathcal{P}_i\boldsymbol{S}_i(1-\tilde{n}_i^d)\mathcal{P}_i, \tag{2.19}$$

which is simply the statement that the presence of a dopon is directly related to a total singlet state while on its absence the only contribution to the total spin $\boldsymbol{J}_i$ comes from

the lattice spin $\boldsymbol{S}_i$. Finally, by the same token, the projected electron occupation number $\tilde{n}_i$ can be written as

$$\tilde{n}_i = \mathcal{P}_i(1 - \tilde{n}_i^d)\mathcal{P}_i. \tag{2.20}$$

Hence, by using the formulas (2.19) and (2.20), the magnetic term H_J in (2.18) can be brought to the form

$$H_J^{\text{enl}} = \sum_{ij} J_{ij} \left(\boldsymbol{S}_i \cdot \boldsymbol{S}_j - \tfrac{1}{4}\right)(1 - \tilde{n}_i^d)(1 - \tilde{n}_j^d) \tag{2.21}$$

which is defined within the enlarged Hilbert space. It is a trivial matter to recognize that due the term $(1 - \tilde{n}_i^d)(1 - \tilde{n}_j^d)$, the given representation for H_J^{enl} vanishes upon acting on the unphysical states (2.4) of $\mathcal{H}^{\text{enl}}$.

Therefore, by collecting the pieces above, we arrive at the Ribeiro and Wen representation of the t-J Hamiltonian in the enlarged Hilbert space

$$\begin{aligned} H_{t\text{-}J}^{\text{enl}} = \sum_{ij} \frac{t_{ij}}{2} \Big[\tilde{d}_i^\dagger \big(\tfrac{1}{2} - \boldsymbol{\sigma} \cdot \boldsymbol{S}_i\big)\big(\tfrac{1}{2} - \boldsymbol{\sigma} \cdot \boldsymbol{S}_j\big)\tilde{d}_j + \text{h.c.}\Big] \\ + \sum_{ij} J_{ij} \left(\boldsymbol{S}_i \cdot \boldsymbol{S}_j - \tfrac{1}{4}\right)(1 - \tilde{n}_i^d)(1 - \tilde{n}_j^d). \end{aligned} \tag{2.22}$$

This concludes our task of rewriting the original model in terms of the spin-dopon operators. In fact, the representation (2.22) provides a different starting point to deal with doped spin models. Although, at first sight it may seem that this is an even more intricate version of the t-J model, the strategy of Ribeiro and Wen consisted in using it as a route to an amenable mean-field treatment of the low doped regime. Because, contrary to the electron density, the dopon density $\delta = \frac{1}{N}\sum_i \langle \tilde{d}_i^\dagger \tilde{d}_i \rangle$ is small at this scenario, where N is the number of lattice sites. Then, being a dilute dopon theory, the no-doubly-occupancy constraint for dopons could be safely relaxed [18].

Unfortunately, as pointed out by Ferraz et al. in [21], their mean-field approximations allowed the participation of the unphysical states (2.4) in the theory. Then, to control such approximations and avoid mixing between both sectors, Ferraz et al. suggested the imposition of a constraint operator into the formalism.

2.4 The Constraint Operator

Due the structure of the proposed map (2.3) between the physical states, the total spin operator $\boldsymbol{J}_i$ can also be used to implement a suitable constraint operator. To do so, let us give a closer look on its properties. First, by using the fact that $\boldsymbol{S}_i^2 = \frac{3}{4}$ and $(\boldsymbol{S}_i^d)^2 = \frac{3}{4}\tilde{n}_i^d$, we can write

$$\boldsymbol{J}_i^2 = \tfrac{3}{4}(1 + \tilde{n}_i^d) + 2\boldsymbol{S}_i \cdot \boldsymbol{S}_i^d. \tag{2.23}$$

In addition to this, we must remember that the physical subspace is made up by either $j = 0$ (vacancy) or $j = \frac{1}{2}$ (lattice site) total spin states. In view of that, we then have

$$\boldsymbol{J}_i^2 \equiv \tfrac{3}{4}(1 - \tilde{n}_i^d), \tag{2.24}$$

which is valid within the physical sector of $\mathcal{H}_i^{\text{enl}}$. Indeed, this last formula allow us to arrive at the desired on-site constraint operator Υ_i proposed by them in [21]. That is, we just need to require that the difference between the formulas (2.23) and (2.24)

$$\Upsilon_i \equiv \frac{1}{2}\Big[\boldsymbol{J}_i^2 - \tfrac{3}{4}(1 - \tilde{n}_i^d)\Big] = \boldsymbol{S}_i \cdot \boldsymbol{S}_i^d + \tfrac{3}{4}\tilde{n}_i^d \tag{2.25}$$

vanishes.[2] Moreover, by inspecting the action of Υ_i on the unphysical (triplet) states (2.4) we can conclude that they are also eigenstates of Υ_i with eingenvalues all equal to one. In a nutshell, we have the remarkable property that

$$\Upsilon_i \left|\text{phys}\right\rangle_i = 0 \qquad \text{and} \qquad \Upsilon_i \left|\text{unphys}\right\rangle_i = \left|\text{unphys}\right\rangle_i . \tag{2.26}$$

As one can see from these results, we could now redefine the on-site projection operator through the simple relation $\mathcal{P}_i = 1 - \Upsilon_i$ [20].

2.5 An Effective Formulation of the t-J Hamiltonian

At this point, one may clearly see the reason of our adopted construction. Since the representation (2.22) for $H_{t\text{-}J}^{\text{enl}}$ vanishes every time it acts on a configuration with unphysical states, one can safely exploit the property (2.26) of the constraint operator Υ_i

[2] The extra $\frac{1}{2}$ factor on the formula was introduced for later convenience.

to dinamically eliminate the unphysical states without the use of the on-site projectors. In this way, we may recast the t-J model as

$$H_{t\text{-}J} = \sum_{ij} \frac{t_{ij}}{2} \Big[\tilde{d}_i^\dagger \big(\tfrac{1}{2} - \boldsymbol{\sigma}\cdot\boldsymbol{S}_i\big)\big(\tfrac{1}{2} - \boldsymbol{\sigma}\cdot\boldsymbol{S}_j\big)\tilde{d}_j + \text{h.c.}\Big] + \sum_{ij} J_{ij}\left(\boldsymbol{S}_i\cdot\boldsymbol{S}_j - \tfrac{1}{4}\right)(1-\tilde{n}_i^d)(1-\tilde{n}_j^d) + \lambda\Upsilon, \qquad (2.27)$$

where $\Upsilon = \sum_j \Upsilon_j$ and the introduced Lagrange multiplier λ is meant to be sent to $+\infty$ at the end of calculations. This is a necessary step to keep the unphysical states unreachable even for the virtual (off-shell) processes that may appear on the field formulation.[3] In other words, although the representation (2.27) for $H_{t\text{-}J}$ now acts in the enlarged Hilbert space $\mathcal{H}^{\text{enl}} = \mathcal{H}^{\text{phys}} \oplus \mathcal{H}^{\text{unphys}}$, the unphysical states are kept apart from the physical sector by a large energy gap of order λ, Figure 2.1.

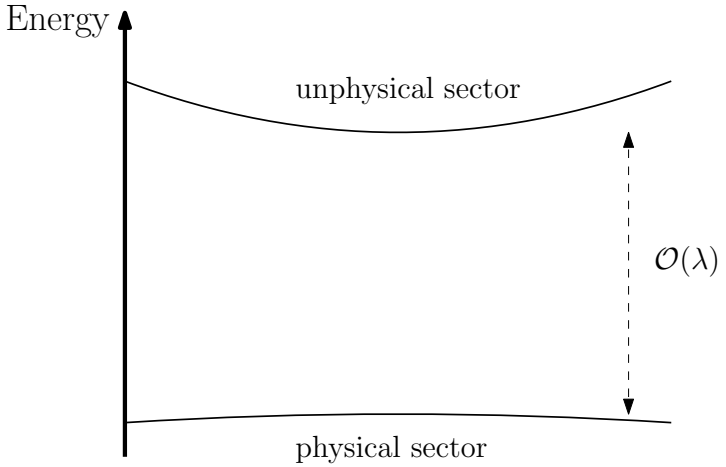

Figure 2.1: Picture portraying the large energy gap exploited to dinamically eliminate the unphysical states of the theory.

As discussed earlier, close to half-filling there will be a small dopon density $\delta \ll 1$, and the no-doubly-occupancy constraint for the dopons can be relaxed in this regime. We can then safely drop the Gutzwiller projection of the dopon operators in the Hamiltonian

[3] Notice the difference between the adopted approach and the standard one:

$$\prod_j \delta(\Upsilon_j) \equiv \int \mathcal{D}\lambda \; e^{i\sum_j \lambda_j \Upsilon_j},$$

which introduces Lagrange multiplier fields that are integrated out. The latter only implies that the constraint $\Upsilon_i = 0$ will be satisfied by the equations of motion without any ensurance of what happens to the off-shell processes.

(2.27) to arrive at the following effective representation

$$H_{t\text{-}J} = \sum_{ij} \frac{t_{ij}}{2} \Big[d_i^\dagger \big(\tfrac{1}{2} - \boldsymbol{\sigma}\cdot\boldsymbol{S}_i\big)\big(\tfrac{1}{2} - \boldsymbol{\sigma}\cdot\boldsymbol{S}_j\big) d_j + \text{h.c.} \Big] \\ + \sum_{ij} J_{ij} \left(\boldsymbol{S}_i\cdot\boldsymbol{S}_j - \tfrac{1}{4}\right)(1-n_i^d)(1-n_j^d) + \lambda \sum_i \Big(\boldsymbol{S}_i\cdot\boldsymbol{S}_i^d + \tfrac{3}{4} n_i^d\Big). \quad (2.28)$$

This last Hamiltonian now acts on a full (unrestricted) spin-dopon Hilbert space which includes the states of the enlarged Hilbert space and the doubly occupied states of dopons as well, i.e., $\mathcal{H}^{\text{full}} = \prod_i \mathcal{H}_i^{\text{full}}$ where

$$\mathcal{H}_i^{\text{full}} = \{ \underbrace{|\Uparrow 0\rangle_i\,, |\Downarrow 0\rangle_i\,, \tfrac{|\Uparrow\downarrow\rangle_i - |\Downarrow\uparrow\rangle_i}{\sqrt{2}}}_{\text{physical states}}, \underbrace{|\Uparrow\uparrow\rangle_i\,, \tfrac{|\Uparrow\downarrow\rangle_i + |\Downarrow\uparrow\rangle_i}{\sqrt{2}}, |\Downarrow\downarrow\rangle_i\,, |\Uparrow\uparrow\downarrow\rangle_i\,, |\Downarrow\uparrow\downarrow\rangle_i}_{\text{unphysical states}} \}. \quad (2.29)$$

As before, we must take the limit $\lambda \to \infty$ at the end of the computations to keep the whole procedure consistent.

One should be careful with that since this last step is highly non-trivial and could mess up with the constraint operator Υ_i defined on (2.25). Miraculously, this is not the case. When we replaced the Gutzwiller projected operators by the full Hilbert space ones, the constraint also changed

$$\Upsilon_i \;\to\; \Upsilon_i = \boldsymbol{S}_i\cdot\boldsymbol{S}_i^d + \tfrac{3}{4} n_i^d, \quad (2.30)$$

in such way that the properties on (2.26) remained the same. Moreover, the initially forbidden doubly occupied dopon states, can be safely accounted since they are also eigenstates with positively defined eigenvalues,

$$\Big(\boldsymbol{S}_i\cdot\boldsymbol{S}_i^d + \tfrac{3}{4} n_i^d\Big)\,|\sigma\rangle_i \otimes |\uparrow\downarrow\rangle_i = \tfrac{3}{2}\,|\sigma\rangle_i \otimes |\uparrow\downarrow\rangle_i\,. \quad (2.31)$$

Remember that this was a crucial property to set apart the unphysical states from the physical ones by a large energy gap.

Finally, we emphasize that a similar effective Hamiltonian description for the t-J model was first proposed by Pepino et al. [20]. Here the difference lies in the the adopted representation for the hopping term H_t^{enl}. The equivalence between such different representations will also be explored in the following chapter.

Chapter 3

Physical Properties of the Spin-Dopon Formulation

This chapter is devoted to study some physical properties of the proposed Hamiltonian (2.28). First, in order to validate this representation, we are going to present a few exact results for simple posed problems which can be directly compared with the results of the original projected electron formulation. Then, at the end, we discuss some physical implications related to the possibility of describing the cuprates through a Kondo-Heisenberg lattice model.

3.1 Some Exact Results

To verify whether the Hamiltonian (2.28) is in fact a bona fide representation of the t-J model, let us solve two rather simple problems which, nevertheless, still encode some underlying physical significance. To test the existence of strong correlations, we inspect its single-site partition function, whereas the role played by the hopping term representation is examined through a two-site problem.

3.1.1 Single-Site Partition Function

Since the physical regime is reached in the limit $\lambda \to \infty$, one may be pushed to face the remaining terms in the Hamiltonian (2.28) as perturbations in comparison to the seemingly dominant term $\lambda\Upsilon$. Adopting this point of view, we may start inspecting the single-site properties of the spin-dopon system. Making use of the grand-canonical

ensemble, the partition function of the theory at this "zeroth order" will be given by

$$\mathcal{Z}_o = \operatorname{tr} e^{-\beta H_o}. \tag{3.1}$$

Here, we already have introduced a chemical potential μ for the dopons in the definition of the Hamiltonian H_o, such that

$$H_o = \lambda \Upsilon - \mu \sum_i n_i^d. \tag{3.2}$$

In the absence of interactions, the partition function of the theory can be factorized as a product of single-site partition functions: $\mathcal{Z}_o = (\mathcal{Z}_{\text{1-site}})^N$, where N is the number of lattice sites as always. This single-site partition function is then obtained by computing its trace using the states of the full spin-dopon Hilbert space in (2.29). The result is

$$\mathcal{Z}_{\text{1-site}}(\zeta, \beta) = 2 + \zeta + 3\zeta e^{-\beta\lambda} + 2\zeta^2 e^{-\frac{3}{2}\beta\lambda}, \tag{3.3}$$

where $\zeta = e^{\beta\mu}$ is the fugacity.

Once we have determined the partition function, we can extract from it all the relevant thermodynamic information of the system. In our present context, this means that we can unravel some physical properties dictated by the constraint operator. Let us begin with the average internal energy per site

$$u_o(\zeta, \beta) = -\left(\frac{\partial}{\partial\beta} \log \mathcal{Z}_{\text{1-site}}\right)_\zeta = \frac{3\zeta\lambda\big(e^{-\beta\lambda} + \zeta e^{-\frac{3}{2}\beta\lambda}\big)}{2 + \zeta\big(1 + 3e^{-\beta\lambda}\big) + 2\zeta^2 e^{-\frac{3}{2}\beta\lambda}}. \tag{3.4}$$

Another quantity of interest for us is the average number of dopons per site

$$\delta_o(\zeta, \beta) = \left(\zeta\frac{\partial}{\partial\zeta} \log \mathcal{Z}_{\text{1-site}}\right)_\beta = \frac{\zeta\big(1 + 3e^{-\beta\lambda}\big) + 4\zeta^2 e^{-\frac{3}{2}\beta\lambda}}{2 + \zeta\big(1 + 3e^{-\beta\lambda}\big) + 2\zeta^2 e^{-\frac{3}{2}\beta\lambda}}. \tag{3.5}$$

Hence, by applying the physical limit $\lambda \to \infty$ in the formulas above, we arrive at the final result:

$$u_o(\zeta, \beta) = 0 \qquad \text{and} \qquad \delta_o(\zeta, \beta) = \frac{1}{1 + 2\zeta^{-1}}. \tag{3.6}$$

This implies that, as expected for a well-defined constraint operator, the ground-state

properties are λ independent. Moreover, given that $u_o = 0$ at this zeroth order, we can see that any finite (and measurable) value for the internal energy of the theory will come from the remaining terms of the Hamiltonian (2.28), which it is worth noting, are all physical.

Although very simple, the results above are really important since they are in accordance with what is expected from a truly strongly correlated system. Just as a short reminder, in the original projected electron formulation the single-site Hamiltonian reads $H = -\mu X^{00}$, where $X^{00} \equiv |0\rangle\langle 0|$ stands for the on-site vacancy number operator.[1] It turns out that within the on-site Hilbert space $\mathcal{H}_{t\text{-}J}$ given in (1.3), the operator X^{00} is represented by a 3×3 matrix with eigenvalues 1, 0 and 0. The associated single-site partition function is then simply given by

$$\mathcal{Z}_{\text{1-site}}(\zeta, \beta) = 2 + \zeta, \tag{3.7}$$

which is precisely the same partition function found on (3.3) in the limit $\lambda \to \infty$ as it should be. Indeed it is a trivial matter to show that (3.7) leads us to the same expressions for the thermodynamical observables u_o and δ_o in (3.6). This implies that the presence of the constraint operator in the effective model (2.28) is crucial to dinamically generate the strong correlations and, therefore, to arrive at the correct results.

A Comment on Regularization

Given that λ is a global parameter, a reader familiar with quantum field theory problems might be inclined to dismiss the $\frac{3}{4}n_i$ term appearing in Υ through a redefinition of the chemical potential. On doing so, the Hamiltonian (3.2) would be replaced by

$$H_o = \lambda \sum_i \boldsymbol{S}_i \cdot \boldsymbol{S}_i^d - \mu \sum_i n_i^d. \tag{3.8}$$

Proceeding anagolously as before, one finds that the new single-site partition function is now given by

$$\mathcal{Z}_{\text{1-site}}(\zeta, \beta) = 2 + \zeta\left(e^{\frac{3}{4}\beta\lambda} + 3e^{-\frac{1}{4}\beta\lambda}\right) + 2\zeta^2. \tag{3.9}$$

[1] A definition to the Hubbard operators X^{ab} is given at the Appendix A. There, we also included a brief introduction to the $su(2|1)$ coherent-state formalism which will be useful in the discussions presented in the next chapter.

From it, we extract the same quantities as before. The expression for the average internal energy density now reads

$$u_o(\zeta,\beta) = -\frac{\frac{3}{4}\zeta\lambda\left(e^{\frac{3}{4}\beta\lambda} - e^{-\frac{1}{4}\beta\lambda}\right)}{2+\zeta\left(e^{\frac{3}{4}\beta\lambda}+3e^{-\frac{1}{4}\beta\lambda}\right)+2\zeta^2}, \tag{3.10}$$

while the dopon density becomes

$$\delta_o(\zeta,\beta) = \frac{\zeta\left(e^{\frac{3}{4}\beta\lambda}+3e^{-\frac{1}{4}\beta\lambda}\right)+4\zeta^2}{2+\zeta\left(e^{\frac{3}{4}\beta\lambda}+3e^{-\frac{1}{4}\beta\lambda}\right)+2\zeta^2}. \tag{3.11}$$

However, this time, in the limit $\lambda \to \infty$ the formulas above gives us that

$$u_o(\zeta,\beta) = -\tfrac{3}{4}\lambda \qquad \text{and} \qquad \delta_o(\zeta,\beta) = 1. \tag{3.12}$$

Differently from the previous results in (3.6), the "new" ground-state properties are physically incompatible with the t-J model. First of all, the ground-state energy is now badly divergent. Second, the dopon density is given by a constant independent of the chemical potential (Fermi energy). That is, in removing the term $\frac{3}{4}n_i$ from Υ the ground-state of the theory has changed and is now made up by singlets at every lattice site available. From this perspective, the term $\frac{3}{4}\lambda n_i$ can be thought of as a sort of heavy Pauli-Villars regulator which is needed to keep this theory finite and consistent.

3.1.2 The Two-Site Problem

Now we move forward to study the role of the hopping term representation in determining the ground-state properties of the spin-dopon $H_{t\text{-}J}$. To gain an intuition on this matter, let us solve a two-site problem using the two different representations for H_t^{enl} given in the previous chapter.

Dopon Hopping Term

Let us start with the purely dopon representation given in equation (2.17). In this case, the Hamiltonian of the problem can be written as $H = H_t + H_J + \lambda\Upsilon$. Explicitly,

each one of its terms reads

$$H_t = 2t\big(d^\dagger_{1\sigma}d_{2\sigma} + d^\dagger_{2\sigma}d_{1\sigma}\big), \qquad H_J = J\big(\boldsymbol{S}_1\cdot\boldsymbol{S}_2 - \tfrac{1}{4}\big)(1-n_1)(1-n_2)$$

$$\text{and} \qquad \Upsilon = \sum_{i=1,2}\big(\boldsymbol{S}_i\cdot\boldsymbol{S}^d_i + \tfrac{3}{4}n_i\big). \tag{3.13}$$

For instance, let us restrict our forthcoming analisys to a single-dopon scenario. This is done in this way because the no dopon case is just a two-site Heisenberg model, and the two dopon scenario corresponds to an overdoped regime ($\delta = 1$) which is far away from our regime of interest. Hence, the Hilbert space for this quantum mechanical problem will be spanned by the following 16 states:

$$\big\{\,|s\rangle\otimes|\sigma 0\rangle\,, |t_n\rangle\otimes|\sigma 0\rangle\,, |\sigma 0\rangle\otimes|s\rangle\,, |\sigma 0\rangle\otimes|t_n\rangle\,\big\}. \tag{3.14}$$

Here we have introduced the shorthand notation $|s\rangle = \frac{|\Uparrow\downarrow\rangle - |\Downarrow\uparrow\rangle}{\sqrt{2}}$ to denote the singlet state and $|t_0\rangle = \frac{|\Uparrow\downarrow\rangle + |\Downarrow\uparrow\rangle}{\sqrt{2}}$, $|t_+\rangle = |\Uparrow\uparrow\rangle$ and $|t_-\rangle = |\Downarrow\downarrow\rangle$ for the triplet states.

To construct a suitable matrix representation for H, we will consider how it acts on each one of the basis states (3.14). Take the constraint operator to begin with. From its fundamental properties in equation (2.26), we get that

$$\Upsilon\,|s\rangle\otimes|\sigma 0\rangle = \Upsilon\,|\sigma 0\rangle\otimes|s\rangle = 0 \qquad \text{and} \qquad \Upsilon\,|t_n\rangle\otimes|\sigma 0\rangle = \Upsilon\,|\sigma 0\rangle\otimes|t_n\rangle = 1. \tag{3.15}$$

A nice simplification comes from the fact that the magnetic term H_J vanishes for the present scenario due to the term $(1-n_1)(1-n_2)$. This fact could be foreseen, since a single dopon living in a two-site lattice is equivalent to a single electron scenario with no other electron to interact magnetically with. Finally, for the dopon hopping term in the equation (3.13), we obtain

$$H_t\,|s\rangle\otimes|\Uparrow 0\rangle = t\,|\Uparrow 0\rangle\otimes|s\rangle + t\,|\Uparrow 0\rangle\otimes|t_0\rangle - t\sqrt{2}\,|\Downarrow 0\rangle\otimes|t_+\rangle\,,$$

$$H_t\,|s\rangle\otimes|\Downarrow 0\rangle = t\,|\Downarrow 0\rangle\otimes|s\rangle - t\,|\Downarrow 0\rangle\otimes|t_0\rangle + t\sqrt{2}\,|\Uparrow 0\rangle\otimes|t_-\rangle\,,$$

$$H_t\,|t_0\rangle\otimes|\Uparrow 0\rangle = t\,|\Uparrow 0\rangle\otimes|s\rangle + t\,|\Uparrow 0\rangle\otimes|t_0\rangle + t\sqrt{2}\,|\Downarrow 0\rangle\otimes|t_+\rangle\,,$$

$$H_t\,|t_0\rangle\otimes|\Downarrow 0\rangle = -t\,|\Downarrow 0\rangle\otimes|s\rangle + t\,|\Downarrow 0\rangle\otimes|t_0\rangle + t\sqrt{2}\,|\Uparrow 0\rangle\otimes|t_-\rangle\,,$$

$$H_t\,|t_+\rangle\otimes|\Uparrow 0\rangle = 2t\,|\Uparrow 0\rangle\otimes|t_+\rangle\,,$$

$$H_t\,|t_+\rangle\otimes|\Downarrow 0\rangle = -t\sqrt{2}\,|\Uparrow 0\rangle\otimes|s\rangle + t\sqrt{2}\,|\Uparrow 0\rangle\otimes|t_0\rangle\,,$$

$$H_t\,|t_-\rangle\otimes|\Uparrow 0\rangle = t\sqrt{2}\,|\Downarrow 0\rangle\otimes|s\rangle + t\sqrt{2}\,|\Downarrow 0\rangle\otimes|t_0\rangle \qquad \text{and}$$

$$H_t\,|t_-\rangle\otimes|\Downarrow 0\rangle = 2t\,|\Downarrow 0\rangle\otimes|t_-\rangle\,. \tag{3.16}$$

We then adopt the following identification for the basis states:

$$|s\rangle\otimes|\Uparrow 0\rangle \equiv \Big(1\ \ 0\ \ 0\ \ 0\ \ 0\ \ 0\ \ 0\ \ 0\ \ |\ \ \mathbf{0}\Big)^T,$$

$$|s\rangle\otimes|\Downarrow 0\rangle \equiv \Big(0\ \ 1\ \ 0\ \ 0\ \ 0\ \ 0\ \ 0\ \ 0\ \ |\ \ \mathbf{0}\Big)^T,$$

$$|t_0\rangle\otimes|\Uparrow 0\rangle \equiv \Big(0\ \ 0\ \ 1\ \ 0\ \ 0\ \ 0\ \ 0\ \ 0\ \ |\ \ \mathbf{0}\Big)^T,$$

$$|t_0\rangle\otimes|\Downarrow 0\rangle \equiv \Big(0\ \ 0\ \ 0\ \ 1\ \ 0\ \ 0\ \ 0\ \ 0\ \ |\ \ \mathbf{0}\Big)^T,$$

$$|t_+\rangle\otimes|\Uparrow 0\rangle \equiv \Big(0\ \ 0\ \ 0\ \ 0\ \ 1\ \ 0\ \ 0\ \ 0\ \ |\ \ \mathbf{0}\Big)^T,$$

$$|t_+\rangle\otimes|\Downarrow 0\rangle \equiv \Big(0\ \ 0\ \ 0\ \ 0\ \ 0\ \ 1\ \ 0\ \ 0\ \ |\ \ \mathbf{0}\Big)^T,$$

$$|t_-\rangle\otimes|\Uparrow 0\rangle \equiv \Big(0\ \ 0\ \ 0\ \ 0\ \ 0\ \ 0\ \ 1\ \ 0\ \ |\ \ \mathbf{0}\Big)^T \qquad \text{and}$$

$$|t_-\rangle\otimes|\Downarrow 0\rangle \equiv \Big(0\ \ 0\ \ 0\ \ 0\ \ 0\ \ 0\ \ 0\ \ 1\ \ |\ \ \mathbf{0}\Big)^T, \tag{3.17}$$

where we have used $\mathbf{0} = \big(0\ \ 0\ \ 0\ \ 0\ \ 0\ \ 0\ \ 0\ \ 0\big)$ for notational simplicity. The remaining states were defined analogously. After that, the Hamiltonian H can be brought to the form of a 16×16 matrix

$$H \equiv \begin{pmatrix} u & v \\ v & u \end{pmatrix}, \tag{3.18}$$

where u and v are 8×8 symmetric matrices. From the results in (3.15), it follows that

$$u = \mathrm{diag}(0, 0, \underbrace{\lambda, \lambda, \lambda, \lambda, \lambda, \lambda}_{6}), \tag{3.19}$$

whereas from (3.16), we get that

$$v = \begin{pmatrix} t & 0 & t & 0 & 0 & -t\sqrt{2} & 0 & 0 \\ 0 & t & 0 & -t & 0 & 0 & t\sqrt{2} & 0 \\ t & 0 & t & 0 & 0 & t\sqrt{2} & 0 & 0 \\ 0 & -t & 0 & t & 0 & 0 & t\sqrt{2} & 0 \\ 0 & 0 & 0 & 0 & 2t & 0 & 0 & 0 \\ -t\sqrt{2} & 0 & t\sqrt{2} & 0 & 0 & 0 & 0 & 0 \\ 0 & t\sqrt{2} & 0 & t\sqrt{2} & 0 & 0 & 0 & 0 \\ 0 & 0 & 0 & 0 & 0 & 0 & 0 & 2t \end{pmatrix}. \tag{3.20}$$

Now, we are able to determine the eigenenergies from the characteristic equation: $\det(H - \varepsilon I_{16\times 16}) = 0$. We then find the 16 energy eigenvalues in the form

$$\varepsilon_n = \left\{ \pm 2t + \lambda,\ \tfrac{1}{2}\left(\lambda \pm \sqrt{\lambda^2 - 4t\lambda + 16t^2}\right),\ \tfrac{1}{2}\left(\lambda \pm \sqrt{\lambda^2 + 4t\lambda + 16t^2}\right) \right\}, \tag{3.21}$$

where, for each sign choice, the first eigenvalue formula in the right-hand side has multiplicity four and each one of the others has multiplicity two. In Figure 3.1, we plot the functional behavior of these eigenenergies with respect to λ.

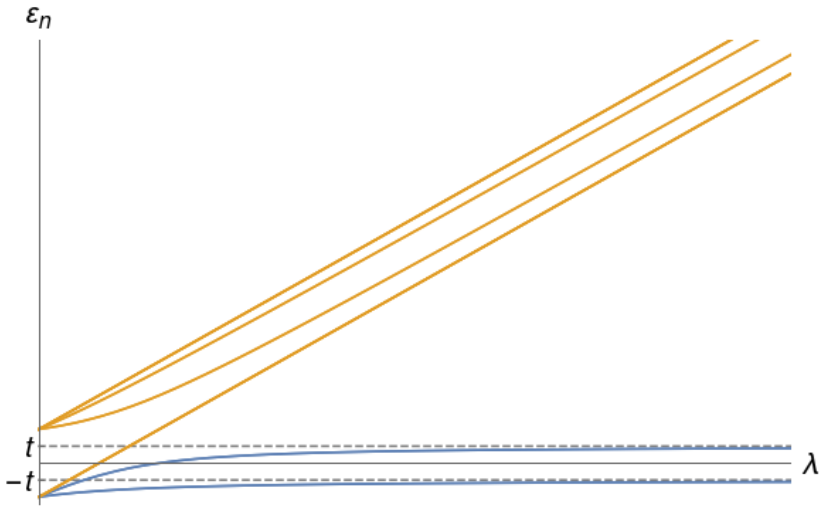

Figure 3.1: Functional behavior of the eigenenergies ε_n in (3.21) with respect to the parameter λ. Notice the separation gap between the physical (blue) and unphysical (orange) sectors in the $\lambda \gg t$ limit.

Then, (by considering $t > 0$) it follows from these results that the ground-state energy is equal to

$$\varepsilon_{\rm GS} = \lim_{\lambda/t\to\infty} \tfrac{1}{2}\Big(\lambda - \sqrt{\lambda^2 + 4t\lambda + 16t^2}\Big) = -t, \tag{3.22}$$

and it is doubly degenerated as mentioned above. This is precisely what is expected from the original t-J model. By setting $t = 1$ for simplify matters, the corresponding ground-state $|\mathrm{GS}\rangle$ is given by the linear combination of the (unnormalized) vectors

$$\begin{aligned}|\mathrm{GS}_{\Uparrow}\rangle = \frac{g(\lambda)}{\sqrt{2}}\Big(\,|s\rangle\otimes|\Uparrow 0\rangle - |\Uparrow 0\rangle\otimes|s\rangle\,\Big) + \frac{1}{\sqrt{2}}\Big(\,|t_0\rangle\otimes|\Uparrow 0\rangle - |\Uparrow 0\rangle\otimes|t_0\rangle\,\Big)\\ - \Big(\,|t_+\rangle\otimes|\Downarrow 0\rangle - |\Downarrow 0\rangle\otimes|t_+\rangle\,\Big)\end{aligned} \tag{3.23}$$

and

$$\begin{aligned}|\mathrm{GS}_{\Downarrow}\rangle = \frac{g(\lambda)}{\sqrt{2}}\Big(\,|s\rangle\otimes|\Downarrow 0\rangle - |\Downarrow 0\rangle\otimes|s\rangle\,\Big) - \frac{1}{\sqrt{2}}\Big(\,|t_0\rangle\otimes|\Downarrow 0\rangle - |\Downarrow 0\rangle\otimes|t_0\rangle\,\Big)\\ + \Big(\,|t_-\rangle\otimes|\Uparrow 0\rangle - |\Uparrow 0\rangle\otimes|t_-\rangle\,\Big),\end{aligned} \tag{3.24}$$

where $g(\lambda) = \frac{1}{2}\big(2+\lambda+\sqrt{16+4\lambda+\lambda^2}\big)$. However since $g(\lambda)\sim\lambda$, for $\lambda \gg 1$, it is easy to conclude that, after a λ-factor normalization procedure, the ground-state eigenstate can be approximated by

$$|\mathrm{GS}\rangle \simeq \frac{\alpha_1}{\sqrt{2}}\Big(\,|s\rangle\otimes|\Uparrow 0\rangle - |\Uparrow 0\rangle\otimes|s\rangle\,\Big) + \frac{\alpha_2}{\sqrt{2}}\Big(\,|s\rangle\otimes|\Downarrow 0\rangle - |\Downarrow 0\rangle\otimes|s\rangle\,\Big). \tag{3.25}$$

where α_1, α_2 are complex constants satisfying the condition $|\alpha_1|^2+|\alpha_2|^2 = 1$. This implies that, even though the representation (2.17) used for the hopping term mixes unphysical and physical subsectors of the theory, the use of the constraint operator $\lambda\Upsilon$ eliminates the unphysical sector of the model, as it should be.

Vacancy Hopping Term

This time we use the vacancy hopping term discussed in the previous chapter and employed in the effective Hamiltonian (2.28). Aside from the hopping term, the remaining terms of the two-site Hamiltonian H defined in (3.13) are still the same. Then, we just

need to verify the action of the vacancy hopping term (2.14) on the basis states (3.14) as before. Thanks to its operational properties, see for example the equation (2.15) and the discussion therein, we obtain a much simpler result:

$$H_t\,|s\rangle \otimes |\Uparrow 0\rangle = t\,|\Uparrow 0\rangle \otimes |s\rangle\,, \qquad H_t\,|s\rangle \otimes |\Downarrow 0\rangle = t\,|\Downarrow 0\rangle \otimes |s\rangle\,,$$

$$\text{and} \qquad H_t\,|t_n\rangle \otimes |\Uparrow 0\rangle = H_t\,|t_n\rangle \otimes |\Downarrow 0\rangle = 0. \tag{3.26}$$

Following the same procedure as before, we arrive again at a 16×16 matrix form like the one presented in (3.18) for H. Although its u component is still given by (3.19), now its v component will be drastically simpler than the one obtained previously,

$$v = \text{diag}(t, t, \underbrace{0, 0, 0, 0, 0, 0}_{6}). \tag{3.27}$$

The computation of the eigenenergies is straightforward and yields us that

$$\varepsilon_n = u_n \pm |v_n| \qquad \text{for} \qquad n = 1, \ldots, 8. \tag{3.28}$$

From this we can get at once the doubly degenerated ground-state energy $\varepsilon_{\text{GS}} = -t$, as expected. However, differently from before, its ground-state wave function is free of unphysical triplet states independently of the scale of the parameter λ,

$$|\text{GS}\rangle = \frac{\alpha_1}{\sqrt{2}}\Big(\,|s\rangle \otimes |\Uparrow 0\rangle - |\Uparrow 0\rangle \otimes |s\rangle\,\Big) + \frac{\alpha_2}{\sqrt{2}}\Big(\,|s\rangle \otimes |\Downarrow 0\rangle - |\Downarrow 0\rangle \otimes |s\rangle\,\Big). \tag{3.29}$$

Such that, $|\text{GS}\rangle$ is an exact eigenstate of the two-site Hamiltonian H with the vacancy hopping term. By means of the map (2.3) between the physical states on both formulations, we can recast $|\text{GS}\rangle$ into the original electron picture as

$$|\text{GS}\rangle = \frac{\alpha_1}{\sqrt{2}}\Big(\,|0\rangle \otimes |\uparrow\rangle - |\uparrow\rangle \otimes |0\rangle\,\Big) + \frac{\alpha_2}{\sqrt{2}}\Big(\,|0\rangle \otimes |\downarrow\rangle - |\downarrow\rangle \otimes |0\rangle\,\Big). \tag{3.30}$$

Under the light of these last results, we see that (despite some algebraic differences) both hopping representations can yield the correct results at the end of the day.

3.1.3 About the Role of the Constraint Operator

As we were able to verify in our calculation of the single-site partition function $\mathcal{Z}_{\text{1-site}}$, the presence of the constraint operator $\lambda\Upsilon$ together with the limit $\lambda \to \infty$ were essential to produce the correct results. Therefore, if we had removed Υ from the Hamiltonian (by taking $\lambda \to 0$ for example), we would have arrived at unphysical results for the partition function and, consequently, for all the resulting thermodynamical quantities. At this point, it is worthwhile to remember that, by taking out the constraint operator of the effective model (2.28), we would arrive at the same Hamiltonian proposed by Ribeiro and Wen [18].

Nevertheless, in the two-site problem with a vacancy hopping term, the existence of $\lambda\Upsilon$ in the Hamiltonian seems to not play any active role on determining the correct (physical) ground-state of the system. As one can readily verify from the formula (3.28) for the eigenenergies, the degeneracy and energy of the ground-state does not change by making $\lambda \to 0$. Thus, while just the Ribeiro and Wen Hamiltonian is not enough to produce the correct partition function in a full spin-dopon Hilbert space. The results obtained indicate that, thanks to its property of non-mixing unphysical and physical subsectors of the theory, their Hamiltonian, notwithstanding, is capable of produce the correct ground-state properties of the system.

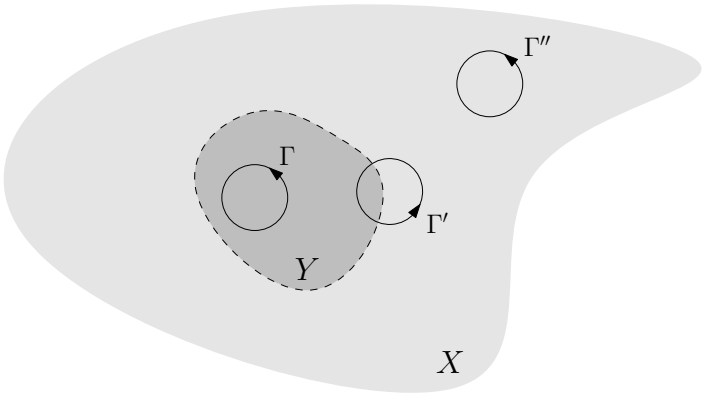

Figure 3.2: Representation of different orbits contributing to the evaluation of the partition function. Here the physical space Y (dark grey area) is embedded into an enlarged space X (light grey area), $Y \subset X$.

Those findings seem to open the possiblity of using a Feynman path integral representation for the quantum partition function of the system. Under this formulation, the quantum thermodynamics is represented by a sum over closed trajectories which obey either periodic or anti-periodic boundary conditions depending on the nature of the ex-

citation described. Let us take for instance, the orbits depicted schematically in Figure 3.2. Trajectories like Γ'' and Γ' are eliminated due the existence of $\lambda\Upsilon$ in the Hamiltonian (2.28) which gives a vanishing statistical weight ($e^{-\lambda\Upsilon} \to 0$ whenever $\Upsilon > 0$) eliminating such unphysical contributions. In particular, Γ'-like trajectories do not exist in the present formulation since the adopted Hamiltonian does not connect the physical and unphysical subsectors of the enlarged Hilbert space. In this way, the only trajectories left are the physical ones (represented by Γ in the Figure 3.2).

3.2 Physical Implications of the Effective Model

Having finished our digression about the faithfulness of the proposed model (2.28), we now turn to the discussion of the physical consequences of such Kondo-Heisenberg lattice Hamiltonian realization of the t-J model.

Perhaps the physical systems which first come to mind when talking about Kondo lattice models are the heavy-fermion compounds [22]. Those other materials of strongly correlated electronic nature are composed of localized magnetic moments which, by being so heavily entangled with the surrounding conduction electrons, profoundly transform the usually expected metallic properties. Their most notorious characteristic (from which their name originates) are the quasiparticle effective masses with a magnitude of up to one thousand times larger than the bare electron mass. Apart from that, heavy-fermion systems can also develop a variety of physical phenomena such as non-Fermi liquid behaviour, different sorts of quantum ordering and unconventional superconductivity.

Hence, the use of the effective Hamiltonian (2.28) suggests an exciting connection between some of the physics of heavy-fermion compounds and the high-T_c cuprates. This reinforces earlier suggestions of a common magnetically mediated mechanism for superconductivity in both heavy-fermion compounds and in the cuprates [23, 24]. Despite these similarities though, we must emphasize that contrary to the heavy-fermions systems which may admit perturbative approaches to the Kondo interaction in some of its regimes, in our present context the coupling λ should always be taken at an incredibly strong coupling regime, i.e. $\lambda \gg t, J$, making any conventional perturbative approach totally unreasonable. One consequence of that is the emergence of different energy scales, which may turn out to be a possible explanation for the difference in the upper bound of

the critical SC transition temperature T_c oberved in these compounds [20].[2]

Another appealing feature of this effective formulation is related to an explanation it may offer for the crossover between the regimes of small and large FS observed experimentally. In the underdoped regime, the only itinerant fermionic degrees of freedom available in the system are the dopons, and since there is just a δ density of them, the generated FS can only account for a Luttinger volume characterized by such a $n = \delta$ carrier density. However, Oshikawa [25] managed to show (nonperturbatively) that, in a Kondo lattice model, the localized spins eventually integrate themselves with the Fermi sea once a well-behaved FL-like phase sets in. As a consequence, it may turn out to be possible that, after reaching some critical value δ^* for the density of dopant carriers, the lattice spins in the spin-dopon model are brought into the construction of a new large FS with a Luttinger volume corresponding to $n = 1 + \delta$ carriers density.

[2]The heavy-fermions materials display a much lower T_c than the one observed on cuprates.

Chapter 4

An Effective Field Theory for Strongly Correlated Electrons

In this chapter, we explore the possibility of constructing a path integral representation for the t-J partition function in terms of spin-dopon variables. Due the severe limitations of the existing methods to treat strongly correlated systems, we introduce an approximation scheme to arrive at an effective description of the model. Finally, we then proceed into its low energy limit by assuming a locally AF environment in (2+1) spacetime dimensions which, in spite of its shortcomings, features small hole-like pockets near the nodal regions of the BZ along with an unconventional mechanism for superconductivity.

4.1 Quantum Partition Function: Field Integral

Due to the projected nature of the canonical t-J Hamiltonian (1.2), many difficulties often arise when representing its partition function by means of a path integral representation. To better see this point, let us make contact with the $su(2|1)$ formulation employed by Ferraz and Kochetov [26] to the original projected electron problem. Let $|z,\xi\rangle$ be a state constructed as a linear combination of the on-site physical states $\frac{|\Uparrow\downarrow\rangle-|\Downarrow\uparrow\rangle}{\sqrt{2}}$, $|\Uparrow 0\rangle$ and $|\Downarrow 0\rangle$, such that it will obviously satisfy the condition $\Upsilon\,|z,\xi\rangle = 0$ as well. Then, in analogy to their construction, the normalizable physical coherent-states of the spin-dopon formulation will take the form

$$|z,\xi\rangle = \frac{\exp\Big(z\,|\Downarrow 0\rangle\,\langle\Uparrow 0| + \xi\frac{|\Uparrow\downarrow\rangle-|\Downarrow\uparrow\rangle}{\sqrt{2}}\,\langle\Uparrow 0|\Big)}{\sqrt{1+\bar{z}z+\bar{\xi}\xi}}\,|\Uparrow 0\rangle = \frac{|\Uparrow 0\rangle + z\,|\Downarrow 0\rangle + \xi\frac{|\Uparrow\downarrow\rangle-|\Downarrow\uparrow\rangle}{\sqrt{2}}}{\sqrt{1+\bar{z}z+\bar{\xi}\xi}}, \quad (4.1)$$

where z and ξ are respectively a complex and a Grassmann parameters. In fact, it is a trivial matter to verify that by using this set of coherent-states along with the spin-dopon Hamiltonian (2.28) to build up the partition function, one will arrive at the exactly same path integral representation found in their work. Within the $su(2|1)$ formulation the resolution of the no-doubly-occupancy constraint for the electrons is encoded into the integration measure, resulting in a rather involved path integral representation.[1] Because of this, it is not yet evident how one can proceed with such a formulation in direct calculations, except in some trivial cases.

Then, let us try an alternative approach motivated by some of the observations made in the previous chapter. In a nutshell, we are going to proceed into an unrestricted spin-dopon path integral representation for the t-J partition function, in which, we are going to use the contraint operator $\lambda\Upsilon$ to identify and, later on, eliminate the unphysical modes of the theory. Introducing sets of spinful fermionic and $SU(2)$ spin coherent states to describe the dopons and lattice spins respectively, we may write the imaginary time field integral of the model as

$$\mathcal{Z} = \int \mathcal{D}\bar{d}\mathcal{D}d\mathcal{D}\boldsymbol{\phi}\; e^{-S[\bar{d},d,\boldsymbol{\phi}]}, \tag{4.2}$$

where its action is given by

$$S[\bar{d},d,\boldsymbol{\phi}] = isS_{\text{WZ}}[\boldsymbol{\phi}] + \int_0^\beta d\tau\Big(L_t[\bar{d},d,\boldsymbol{\phi}] + H_J[\bar{d},d,\boldsymbol{\phi}] + \lambda\Upsilon[\bar{d},d,\boldsymbol{\phi}]\Big). \tag{4.3}$$

Here we use s as the localized spin quantum number, and the functional integration is made over the Grassmannian $\bar{d}_{i\sigma}$, $d_{i\sigma}$ and vector $\boldsymbol{\phi} \in S^2$ fields. The first term appearing in the action is just a sum of single-site Wess-Zumino(-Witten) terms

$$S_{\text{WZ}}[\boldsymbol{\phi}] = \sum_i \int_0^\beta d\tau \int_0^1 d\upsilon\; \boldsymbol{\phi}_i(\tau,\upsilon)\cdot\big[\partial_\tau\boldsymbol{\phi}_i(\tau,\upsilon)\times\partial_\upsilon\boldsymbol{\phi}_i(\tau,\upsilon)\big]. \tag{4.4}$$

Each one of these on-site contributions accounts for the accumulated Berry phase of a particular lattice spin under a closed trajectory in the parameter space. All these trajectories satisfy the following boundary conditions:

$$\boldsymbol{\phi}_i(\tau,0) \equiv \boldsymbol{\phi}_i(\tau), \qquad \boldsymbol{\phi}_i(\tau,1) \equiv \hat{\boldsymbol{z}} \qquad \text{and} \qquad \boldsymbol{\phi}_i(0,\upsilon) = \boldsymbol{\phi}_i(\beta,\upsilon), \tag{4.5}$$

[1] A discussion about the structure of the $su(2|1)$ measure was included at the Appendix A.

where $\tau \in [0, \beta]$ and $\upsilon \in [0, 1]$. Finally, the remaining terms appearing in the expression (4.3) for the action are

$$L_t[\bar{d}, d, \boldsymbol{\phi}] = \sum_i \bar{d}_i(\partial_\tau - \mu)d_i + \sum_{ij} \frac{t_{ij}}{8}\Big[\bar{d}_i\big(1 - \boldsymbol{\sigma}\cdot\boldsymbol{\phi}_i\big)\big(1 - \boldsymbol{\sigma}\cdot\boldsymbol{\phi}_j\big)d_j + \text{h.c.}\Big]$$

$$\text{and} \qquad H_J[\bar{d}, d, \boldsymbol{\phi}] = \sum_{ij} J_{ij}\Big[\tfrac{1}{2}s^2\big(\boldsymbol{\phi}_i + \boldsymbol{\phi}_j\big)^2 - 1\Big](1 - n_i^d)(1 - n_j^d), \tag{4.6}$$

where we have introduced a chemical potential μ for the dopons as well.

This concludes our proposed task of writing a path integral representation for the t-J in terms of spin-dopon variables. At this stage it is helpful to give a closer look into the behavior of the constraint operator inside the spin-dopon path integral. It is obvious that unphysical modes do not contribute onto the partition function since $e^{-\lambda\Upsilon} \to 0$ for any configuration with $\Upsilon > 0$, as emphasized in the previous chapter. Namely, any state characterized by $n_i^d = 0$ and $n_i^d = 2$ gives us

$$\big(\boldsymbol{S}_i \cdot \boldsymbol{S}_i^d + \tfrac{3}{4}n_i^d\big)_{\text{0-dopon}} = 0 \qquad \text{and} \qquad \big(\boldsymbol{S}_i \cdot \boldsymbol{S}_i^d + \tfrac{3}{4}n_i^d\big)_{\text{2-dopon}} > 0, \tag{4.7}$$

which means that they are automatically accounted for or simply eliminated from the final result, as expected. In fact, the intricate (and crucial) part here are the single dopon occupied states which can either form singlet or triplet states with the lattice spins.

4.1.1 The Vacancy Effective Theory

To make further progress, however, we propose an approximate strategy. Let us consider the dopon motion in a slowly varying lattice spin configuration. In this case we may use a semiclassical approach: first we find a static lattice spin configuration which minimizes the energy of the system for a given doping, and then take into account quantum fluctuations around this stationary phase.

To develop some physical intuition within this approximation, let us consider a single dopon hopping from sites i to j. Then, due to its (infinitely) strong Kondo coupling to the lattice spins, the spin of the hopping dopon is forced to align anti-parallel to $\boldsymbol{S}_i$ and $\boldsymbol{S}_j$ at each site.[2] In other words, at every site i where the dopon arrives, its local constraint

[2]This line of reasoning was based on a similar argument given by Ohgushi et al. [27] when studying the strong limit of the Hund's coupling between electrons to localized spins aligned ferromagnetically.

operator needs to satisfy

$$\big(\boldsymbol{S}_i \cdot \boldsymbol{S}_i^d + \tfrac{3}{4}\big)_{\text{1-dopon}} = \tfrac{1}{2}(\boldsymbol{S}_i + \boldsymbol{S}_i^d)^2 = 0. \tag{4.8}$$

to be accounted in the partition function. In the spin coherent-state representation that we have adopted, this simple picture just tell us that given a state

$$|\boldsymbol{\phi}_i\rangle = e^{-i\varphi_i S_i^z} e^{-i\theta_i S_i^y} e^{-i\psi_i S_i^z} \,|\Uparrow_i\rangle = e^{-\frac{i}{2}\psi_i}\Big[e^{-\frac{i}{2}\varphi_i}\cos\big(\tfrac{\theta_i}{2}\big)\,|\Uparrow_i\rangle + e^{\frac{i}{2}\varphi_i}\sin\big(\tfrac{\theta_i}{2}\big)\,|\Downarrow_i\rangle\Big], \tag{4.9}$$

for the localized spin at site i, the physical dopon's spin wave function $\big|\boldsymbol{\phi}_i^d\big\rangle$ at the same lattice site will be locked into the configuration

$$\big|\boldsymbol{\phi}_i^d\big\rangle = ie^{-\frac{i}{2}\psi_i^d}\Big[-e^{-\frac{i}{2}\varphi_i}\sin\big(\tfrac{\theta_i}{2}\big)\,|\uparrow\rangle + e^{\frac{i}{2}\varphi_i}\cos\big(\tfrac{\theta_i}{2}\big)\,|\downarrow\rangle\Big], \tag{4.10}$$

where $\varphi, \psi \in [0, 2\pi)$ and $\theta \in [0, \pi)$ stands for the Euler angles.[3] Then, by using the parametrization given above for the on-site states, it is a trivial matter to show that $\langle\boldsymbol{\phi}_i|\,\boldsymbol{S}_i\,|\boldsymbol{\phi}_i\rangle = \frac{1}{2}\boldsymbol{\phi}_i$, whereas $\big\langle\boldsymbol{\phi}_i^d\big|\,\boldsymbol{S}_i^d\,\big|\boldsymbol{\phi}_i^d\big\rangle = \frac{1}{2}\boldsymbol{\phi}_i^d = -\frac{1}{2}\boldsymbol{\phi}_i$. Hence, it solves the constraint equation (4.8) within this approximation regime.

The Hopping Term

The procedure above tell us that, due to the existence of the constraint operator, the dopon's spin degrees of fredom are in fact redundant and can be written in terms of the lattice spin variables. So let us make use of this information on the dopon's spin wave function to recast the Lagrangian $L_t[\bar{d}, d, \boldsymbol{\phi}]$ in (4.6), as

$$L_t[\bar{\eta}, \eta, \boldsymbol{\phi}] = \sum_i \bar{\eta}_i(\partial_\tau + i\mathcal{A}_i^0 - \mu)\eta_i + \sum_{ij}\big(T_{ij}\bar{\eta}_i\eta_j + \text{h.c.}\big). \tag{4.11}$$

The Grassmannian fields $\bar{\eta}_i$, η_i were introduced to represent the on-site singlets (i.e., vacancies in the original electron picture), and it can be thought of as a remaining spinless piece of the dopon field. This substitution leads to the emergence of an on-site scalar potential $\mathcal{A}_i^0 = -i\,\big\langle\boldsymbol{\phi}_i^d\big|\partial_\tau\boldsymbol{\phi}_i^d\big\rangle$, ultimately related to the lattice spin dynamics,[4] and the

[3] The angles ψ_i and ψ_i^d are related to overall phases and they do not appear in physical observables.

[4] Keep in mind that the dopon spin wave function is written in terms of the lattice spin variables. Once one does that, it is simple to figure out that $\mathcal{A}^0$ has the same structure of a lattice spin Berry phase.

effective vacancy transfer integral T_{ij}, which is given by

$$T_{ij} = \tfrac{1}{4} t_{ij} \left\langle \boldsymbol{\phi}_i^d \right| \big(1 - \boldsymbol{\sigma} \cdot \boldsymbol{\phi}_i\big)\big(1 - \boldsymbol{\sigma} \cdot \boldsymbol{\phi}_j\big) \left| \boldsymbol{\phi}_j^d \right\rangle . \tag{4.12}$$

Evaluting the matrix element above, we find

$$\begin{aligned} &\left\langle \boldsymbol{\phi}_i^d \right| \big(1 - \boldsymbol{\sigma} \cdot \boldsymbol{\phi}_i\big)\big(1 - \boldsymbol{\sigma} \cdot \boldsymbol{\phi}_j\big) \left| \boldsymbol{\phi}_j^d \right\rangle = \\ &\quad = 4\Big[e^{i\phi_j} \cos\!\big(\tfrac{\theta_i}{2}\big) \cos\big(\tfrac{\theta_j}{2}\big) + e^{i\phi_i} \sin\!\big(\tfrac{\theta_i}{2}\big) \sin\big(\tfrac{\theta_j}{2}\big) \Big] e^{\frac{i}{2}(\psi_i^d - \psi_j^d) - \frac{i}{2}(\phi_i + \phi_j)}, \end{aligned} \tag{4.13}$$

such that, the effective transfer integral T_{ij} can also be written as

$$T_{ij} = t_{ij} \Big| e^{i\phi_j} \cos\!\big(\tfrac{\theta_i}{2}\big) \cos\big(\tfrac{\theta_j}{2}\big) + e^{i\phi_i} \sin\!\big(\tfrac{\theta_i}{2}\big) \sin\big(\tfrac{\theta_j}{2}\big) \Big| e^{i\mathcal{A}_{ij}} = t_{ij} \cos\big(\tfrac{\theta_{ij}}{2}\big) e^{i\mathcal{A}_{ij}} \tag{4.14}$$

where θ_{ij} stands for the angle between the two spins $\boldsymbol{\phi}_i$ and $\boldsymbol{\phi}_j$. The linking phase $\mathcal{A}_{ij}$ is a potential vector generated by the lattice spins, and corresponds to the Berry phase felt by the hopping dopon. Although the $\mathcal{A}_{ij}$'s are all gauge dependent quantities, they must satisfy the gauge independent condition

$$\exp(i\Phi) = \prod_C \exp(i\mathcal{A}_{ij}), \tag{4.15}$$

where Φ is the flux threading the surface bounded by the closed lattice contour C. Let us then rewrite the Lagrangian L_t (4.11) in a more convenient way as

$$L_t[\bar{\eta}, \eta, \boldsymbol{\phi}] = \sum_i \bar{\eta}_i (\partial_\tau + i\mathcal{A}_i^0 - \mu)\eta_i + \sum_{ij} \big(\tilde{t}_{ij} \bar{\eta}_i \eta_j e^{i\mathcal{A}_{ij}} + \text{h.c.} \big) \tag{4.16}$$

where $\tilde{t}_{ij} = t_{ij} \cos\big(\frac{\theta_{ij}}{2}\big)$ is a "renormalized" hopping amplitude, which can be thought of as the bare hopping amplitude t_{ij} dressed by the lattice spin background configuration.

Physical Significance of the Emergent Lattice Gauge Field

It seems from the resulting Lagrangian (4.16) that we are dealing with some sort of lattice gauge theory coupled to spinless fermions. To understand the physical meaning of

such a gauge theory, let us inspect the behavior of the topological order operator [28]

$$W(C) = \mathrm{tr} \prod_{i \in C} (\tfrac{1}{2} - \boldsymbol{\sigma} \cdot \boldsymbol{S}_i). \tag{4.17}$$

Here, it is worth noting that a similar operational structure was already present from the very beginning in the hopping term (2.14). Performing a simple calculation for an elementary 3-site loop C_{123}, like the one depicted in Figure 4.1, will lead us to the result

$$W(C_{123}) = \tfrac{1}{4} + \boldsymbol{S}_1 \cdot \boldsymbol{S}_2 + \boldsymbol{S}_2 \cdot \boldsymbol{S}_3 + \boldsymbol{S}_3 \cdot \boldsymbol{S}_1 - 2i(\boldsymbol{S}_1 \times \boldsymbol{S}_2) \cdot \boldsymbol{S}_3. \tag{4.18}$$

However, in order to make contact with observable quantities, we must look up to the difference between going around the loop in the counterclockwise and clockwise directions $W(C_{123}) - W(C_{132}) = -4iE_{123}$, where E_{123} is the spin chirality operator defined as

$$E_{123} = \boldsymbol{S}_1 \cdot (\boldsymbol{S}_2 \times \boldsymbol{S}_3) \tag{4.19}$$

It is well known that such an operator, in general, breaks both parity P and time reversal T symmetries, and plays an important role in chiral spin liquid theory [29, 30].

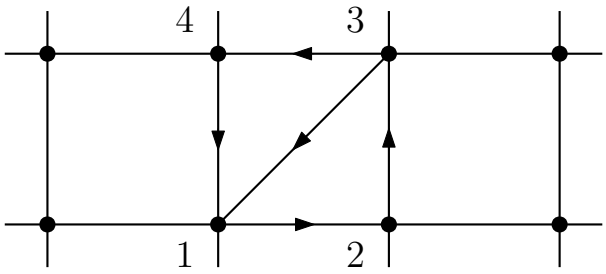

Figure 4.1: Example of elementary 3- and 4-site lattice loops.

On the other hand, it turns out that the expectation value of $W(C)$ acquires the form of a Wilson loop which is tied to the value of the afore mentioned flux Φ through $\langle W(C) \rangle = W_0 \exp i\Phi$. In this way, we are led to conclude that

$$\langle E_{123} \rangle = -\tfrac{1}{2} W_0 \sin \Phi. \tag{4.20}$$

Hence, for values of the flux $\Phi = 0, \pi$ we do not observe neither P nor T symmetry breaking in the theory.

An analogous procedure can be carried over to a 4-site loop C_{1234} which eventually will lead us to the result

$$W(C_{1234}) - W(C_{1432}) = -2i\Big(E_{123} + E_{234} + E_{341} + E_{412}\Big). \tag{4.21}$$

Then again $\big\langle E_{123}+E_{234}+E_{341}+E_{412}\big\rangle = -W_0 \sin\Phi$, where this time Φ is the flux threading through the 4-site loop.

The Effective Action

Thus, after eliminating the dopon's spin degrees of freedom in favor of the lattice spin variables in the remaining terms of the action (4.3), we then arrive at the following effective description of the theory

$$S[\bar{\eta}, \eta, \boldsymbol{\phi}] = isS_{\mathrm{WZ}}[\boldsymbol{\phi}] + \int_0^\beta d\tau \Big(L_t[\bar{\eta}, \eta, \boldsymbol{\phi}] + H_J[\bar{\eta}, \eta, \boldsymbol{\phi}] \Big) \tag{4.22}$$

where the expressions for $S_{\mathrm{WZ}}[\boldsymbol{\phi}]$ and $L_t[\bar{\eta}, \eta, \boldsymbol{\phi}]$ were already given at the equations (4.4) and (4.16), respectively. However the magnetic term H_J now reads

$$H_J[\bar{\eta}, \eta, \boldsymbol{\phi}] = \sum_{ij} J_{ij} \Big[\tfrac{1}{2} s^2 \big(\boldsymbol{\phi}_i + \boldsymbol{\phi}_j\big)^2 - 1 \Big] (1 - \bar{\eta}_i \eta_i)(1 - \bar{\eta}_j \eta_j). \tag{4.23}$$

At this point, it shall be interesting to verify the validity of such a description of the t-J model. For instance, let us examine the case for $J_{ij} = 0$ (i.e., the $U = \infty$ Hubbard model) in one spatial dimension. In this scenario the lattice spins have no dynamics of their own and the configuration which minimizes the energy corresponds to a ferromagnetic arrangement of spins. This is so because the effective hopping amplitude will have its highest value at $\tilde{t}_{ij} = t_{ij}$ provided that $\forall \theta_{ij} = 0$. Considering just nearest neighbor hopping processes, we diagonalize the kinetical piece of the action by going to the momentum space

$$S_t[\bar{\eta}, \eta] = \sum_k \bar{\eta}_k (-i\omega_n + \xi_k) \eta_k \tag{4.24}$$

where $\xi_k = 2t \cos k_x - \mu$ and $k = (i\omega_n, k_x)$. For $t > 0$, the band minima will be located at the corners of the BZ labelled by $k_x = \pm\pi$. Then, provided that k_F is the Fermi

momentum, it follows that the ground-state energy of the system takes the form $\frac{E_{\rm GS}}{N} = -\frac{2t}{\pi}\sin k_F$. In one dimension, we also have that $k_F = \pi(1-\delta) = \pi n_e$, where n_e is the density of electrons.[5] Thus, the final result for the ground-state energy is

$$\frac{E_{\rm GS}}{N} = -\frac{2t}{\pi}\sin(\pi n_e) \tag{4.25}$$

which coincides with the exact result for the $U = \infty$ Hubbard model in one spatial dimension [31, 32].

Apart from this simple problem, the present form of the action $S[\bar{\eta}, \eta, \boldsymbol{\phi}]$ given on (4.22) is still difficult to handle for more involved cases. This difficulty is mainly a consequence of the fact that $\tilde{t}_{ij}$, $\mathcal{A}_i^0$ and $\mathcal{A}_{ij}$ are all implicit functions of the lattice spin variables. To circumvent this, we will recast the spin sector of the theory in terms of an emergent gauge field $\mathcal{A}^\mu$ to derive a low energy effective action of this model in the next section.

4.2 Low Energy Effective Field Theory for an Underdoped AF

To make some touch with the cuprates phenomenology, let us try to derive a low energy effective field theory for the lightly doped regime of (4.22) in (2+1) spacetime dimensions. Thanks to the proximity to the parent AF Mott insulator phase, we begin by assuming the existence of a short range AF order, Figure 1.1. So let us introduce two perpendicular smooth fields $\boldsymbol{n}(\boldsymbol{x}, \tau)$ and $\boldsymbol{l}(\boldsymbol{x}, \tau)$ to represent, respectively, the antiferromagnetic and the ferromagnetic components of the original spin field $\boldsymbol{\phi}(\boldsymbol{x}, \tau)$. Then, we may decompose the lattice spin field as

$$\boldsymbol{\phi}(\boldsymbol{x}_i, \tau) = (-1)^i \boldsymbol{n}(\boldsymbol{x}_i, \tau)\sqrt{1 - \left|a^2 \boldsymbol{l}(\boldsymbol{x}_i, \tau)\right|^2} + a^2 \boldsymbol{l}(\boldsymbol{x}_i, \tau) \tag{4.26}$$

from which follows directly that $|\boldsymbol{\phi}(\boldsymbol{x}_i, \tau)|^2 = |\boldsymbol{n}(\boldsymbol{x}_i, \tau)|^2 = 1$. Since we are interested in arriving at a continuum limit, we perform an expansion in orders of the lattice parameter a, which results in

$$\boldsymbol{\phi}(\boldsymbol{x}_i, \tau) = (-1)^i \boldsymbol{n}(\boldsymbol{x}_i, \tau) + a^2 \boldsymbol{l}(\boldsymbol{x}_i, \tau) + \mathcal{O}(a^4). \tag{4.27}$$

We will then use the ansatz above to inspect the behavior of the effective action

[5] The Fermi momentum k_F is defined with respect the center of the BZ, $k_x \in [-\pi, \pi]$.

(4.22) in the presence of this local AF environment. We first consider the magnetic term $H_J[\bar{\eta}, \eta, \boldsymbol{\phi}]$ given in (4.23). After extracting from it the spin independent contribution $H_I[\bar{\eta}, \eta]$, defined as

$$H_I[\bar{\eta}, \eta] = -J \sum_{\langle ij \rangle} (1 - \bar{\eta}_i \eta_i)(1 - \bar{\eta}_j \eta_j), \tag{4.28}$$

its remaining piece will now read

$$H_{\rm spin}[\bar{\eta}, \eta, \boldsymbol{\phi}] = \frac{Js^2}{2} \sum_{\langle ij \rangle} \big(\boldsymbol{\phi}_i + \boldsymbol{\phi}_j\big)^2 (1 - \bar{\eta}_i \eta_i)(1 - \bar{\eta}_j \eta_j), \tag{4.29}$$

where we have restricted the exchange coupling to first neighbors to simplify our analysis. Looking upon the formula for $H_{\rm spin}[\bar{\eta}, \eta, \boldsymbol{\phi}]$, it is not difficult to verify that $(\boldsymbol{\phi}_i + \boldsymbol{\phi}_j)^2$ will only receive nonzero contributions from fluctuations. This makes it safe to neglect further small corrections from the operator $(1 - \bar{\eta}_i \eta_i)$, and replace it by its average value $(1 - \delta)$. Proceeding in this way, $H_{\rm spin}[\bar{\eta}, \eta, \boldsymbol{\phi}]$ is then reduced to a Heisenberg Hamiltonian

$$H_{\rm spin}[\boldsymbol{\phi}] = \frac{\tilde{J}s^2}{2} \sum_{\langle ij \rangle} \big(\boldsymbol{\phi}_i + \boldsymbol{\phi}_j\big)^2 \tag{4.30}$$

with a renormalized exchange constant $\tilde{J} = (1 - \delta)^2 J$.

4.2.1 The Spin Sector

At this stage, one should have already noticed that the action associated with the spin sector of the theory

$$S_{\rm spin}[\boldsymbol{\phi}] = isS_{\rm WZ}[\boldsymbol{\phi}] + \int_0^\beta d\tau \; H_{\rm spin}[\boldsymbol{\phi}], \tag{4.31}$$

is equivalent to a Heisenberg AF model with an exchange coupling constant $\tilde{J}$. We can then proceed in a standard fashion to determine the continuum dynamics of $S_{\rm spin}[\boldsymbol{\phi}]$ in terms of the smooth field $\boldsymbol{n}(\boldsymbol{x}, \tau)$ [33, 34].[6] Neglecting small ferromagnetic fluctuations coming from $L_t[\bar{\eta}, \eta, \boldsymbol{\phi}]$, we can integrate out the $\boldsymbol{l}(\boldsymbol{x}, \tau)$ field and arrive at the following

[6] To not bother the reader with too much detail, we have included these manipulations, along with an analysis about the role of quantum fluctuations, in Appendix B.

relativistic $O(3)$ non-linear σ model (NLσM):

$$S_{\rm spin}[\boldsymbol{n}] = \frac{1}{2g}\int d^3x \big(c_s^{-1}|\partial_\tau \boldsymbol{n}|^2 + c_s|\nabla \boldsymbol{n}|^2\big), \tag{4.32}$$

where $g = 2\sqrt{2}a/s$ and $c_s = 2\sqrt{2}\tilde{J}sa$ are respectively an effective coupling constant and the spin-wave velocity. Another parameter often found in the condensed matter literature is the spin stiffness $\rho_s = c_s/g = \tilde{J}s^2$. After taking into account quantum fluctuations, we see that indeed the effective action may read

$$S_{\rm spin}[\boldsymbol{n}] = \frac{1}{2g}\int d^3x \left(c_s^{-1}|\partial_\tau \boldsymbol{n}|^2 + c_s|\nabla \boldsymbol{n}|^2 + c_s^3 m^2|\boldsymbol{n}|^2\right). \tag{4.33}$$

Here, for $g > g_c$, the mass parameter $m \sim \xi_s^{-1}$ assumes a finite value and, as a result, the AF order is short ranged. Otherwise, the mass vanishes and the AF order continues to be long ranged ($\xi_s \to \infty$).

Quantum Antiferromagnetism as a Gauge Theory

To proceed further, let us consider the CP^1 representation of the $O(3)$ NLσM. In this description, the field $\boldsymbol{n}$ is related to a two component charged boson $z = \begin{pmatrix} z_1 & z_2 \end{pmatrix}^T$ through the Hopf map $\boldsymbol{n} = z^\dagger \boldsymbol{\sigma} z$. From this it also follows that $\boldsymbol{n}^2 = z^\dagger z = 1$, by using the completeness relation of the Pauli matrices.[7] Then, by using the formulas above, one eventually finds that

$$\partial_\mu \boldsymbol{n} \cdot \partial^\mu \boldsymbol{n} = 4\big[\partial_\mu z^\dagger \partial^\mu z + (z^\dagger \partial_\mu z)^2\big], \tag{4.34}$$

where for notational convenience we have adopted units of $c_s = 1$. Returning to the NLσM action in (4.33), we now have

$$S_{\rm spin}[z^\dagger, z] = \frac{2}{g}\int d^3x \Big[\partial_\mu z^\dagger \partial^\mu z + (z^\dagger \partial_\mu z)^2 + m^2 z^\dagger z\Big]. \tag{4.35}$$

The quartic z term can be simplified, if we introduce an auxiliary Hubbard-Stratonovich

[7] These formulas define a projection of the sphere S^3 in z-space onto a sphere S^2 defined by $\boldsymbol{n}$. The "extra" degree of freedom of (z_1, z_2) is unobservable since it is related to a global phase transformation of the spinor z.

field $\mathcal{A}^\mu$ through the identity

$$e^{-S_{\text{spin}}[z^\dagger,z]} = \int \mathcal{D}\mathcal{A}_\mu \ \exp\Big\{-\frac{2}{g}\int d^3x\Big[\partial_\mu z^\dagger \partial^\mu z + (z^\dagger\partial_\mu z)^2 + m^2 z^\dagger z + \mathcal{A}_\mu\mathcal{A}^\mu\Big]\Big\}, \quad (4.36)$$

and we perform the translation $\mathcal{A}_\mu \to \mathcal{A}_\mu + z^\dagger(-i\partial_\mu)z$. This last procedure leads us to the so called CP^1 action

$$S_{\text{spin}}[z^\dagger, z, \mathcal{A}_\mu] = \frac{2}{g}\int d^3x\Big(|D_\mu z|^2 + m^2|z|^2\Big), \quad (4.37)$$

where $D_\mu = \partial_\mu + i\mathcal{A}_\mu$ is a covariant derivative.

Now, if we just integrate out the z-bosons, neglecting small fluctuations coming from the remaining terms of the action, we get the following gauge effective action

$$S_{\text{spin}}[\mathcal{A}_\mu] = 2\ln\det\Big\{2g^{-1}\Big[(-\partial^2 + m^2) - \mathcal{A}_\mu i\overset{\leftrightarrow}{\partial}_\mu + \mathcal{A}_\mu\mathcal{A}^\mu\Big]\Big\}. \quad (4.38)$$

Then, by restricting the analysis up to quadratic order in terms of the gauge field, we get

$$S_{\text{spin}}[\mathcal{A}_\mu] = \frac{1}{2}\int \frac{d^3q}{(2\pi)^3}\mathcal{A}_\mu(q)\Pi^{\mu\nu}(q)\mathcal{A}_\nu(-q) \quad (4.39)$$

where $\Pi^{\mu\nu}(q) = \big(\delta^{\mu\nu}q^2 - q^\mu q^\nu\big)\Pi(q^2)$ is the one-particle irreducible (1PI) current-current correlation function of the z-bosons with[8]

$$\Pi(q^2) = \frac{1}{2\pi g}\int_0^1 dx \frac{(1-2x)^2}{\sqrt{m^2 + x(1-x)q^2}}. \quad (4.40)$$

In the strongly disordered system, we may perform a gradient expansion in powers of the large mass m to get at leading order the (Wick rotated) Maxwellian term

$$S_{\text{spin}}[\mathcal{A}_\mu] = \frac{1}{4\kappa^2}\int d^3x\ (\mathcal{F}_{\mu\nu})^2 \quad (4.41)$$

with a gauge coupling charge $\kappa = \sqrt{6\pi|m|g}$, and whose field strength tensor reads

$$\mathcal{F}_{\mu\nu} = \partial_\mu\mathcal{A}_\nu - \partial_\nu\mathcal{A}_\mu = \tfrac{1}{2}\boldsymbol{n}\cdot(\partial_\mu\boldsymbol{n}\times\partial_\nu\boldsymbol{n}). \quad (4.42)$$

Thus, the field $\mathcal{A}^\mu$ which originally had no kinetic energy and could have been elimi-

[8]The computational details of this procedure are available in Appendix C.

nated from the CP^1 action (4.37), due to quantum effects, acquires here a real dynamical character. Moreover, by inspecting the formula (4.42) for $\mathcal{F}_{\mu\nu}$ we may notice that it is exactly what the continuum version of the spin chirality operator (4.19) would look like if we were to examine spacetime plaquettes. At this point, we can also perceive that the main effect of the neglected fluctuations from the remaining terms of the action would only be to renormalize the effective charge κ since, by requiring Lorentz invariance, we could still recover a Maxwell Lagrangian at the end of the day.

4.2.2 The Charged Sector

Now we turn our attention to the remaining terms of the effective action in (4.22), $L_t[\bar{\eta}, \eta, \boldsymbol{\phi}]$ and $H_I[\bar{\eta}, \eta]$. As we are going to see, they will amount to a dilute charged sector, which comprises the bare FS structure, a quartic interaction between fermions, and a gauge coupling to the spin sector.

The Bare Fermi Surface

Consider for instance, the term $L_t[\bar{\eta}, \eta, \boldsymbol{\phi}]$ given in equation (4.16), embedded into a static staggered AF configuration. It is not difficult to notice that the renormalized hopping amplitude $\tilde{t}_{ij} = t_{ij} \cos\left(\frac{\theta_{ij}}{2}\right)$ vanishes for processes connecting different Néel sublattices. So, at this level, there is a complete separation between two species of fermions living in different (A and B) sublattices.[9] Let us also assume the simplest non P,T simmetry breaking ground-state characterized by $\Phi = 0$. Then, taking $t_{ij} = t, t', t''$ for first, second and third nearest neighbor hopping amplitudes, we diagonalize this free action term by going to the momentum space $k = (i\omega_n, \boldsymbol{k})$. The result is

$$S_t^{(0)}[\bar{\eta}, \eta] = \sum_{k,a} \bar{\eta}_{k,a}(-i\omega_n + \xi_{\boldsymbol{k}})\eta_{k,a}, \tag{4.43}$$

where $\xi_{\boldsymbol{k}} = 4t' \cos k_x \cos k_y + 2t''\big(\cos 2k_x + \cos 2k_y\big) - \mu$ is the dispersion and $a = \{A, B\}$ is a sublattice flavor label.

As a consequence of that, the dispersion has now the symmetry $\xi_{\boldsymbol{k}} = \xi_{\boldsymbol{k}+(\pi,\pi)}$, and dependending on the sign and relative size of the bare electron parameters t' and t'', the

[9] This might resemble the chiral symmetry of massless Dirac fermions. Analogously to the Gross-Neveu model, the latter inclusion of quartic interactions may induce a mixture of the different fermionic flavors leading to a sort of chiral symmetry breaking.

band minima may be located either at $(0,0)$, $\{(\pm\pi,0),(0,\pm\pi)\}$ or at $\{(\pm\frac{\pi}{2},\frac{\pi}{2}),(\pm\frac{\pi}{2},-\frac{\pi}{2})\}$ within the magnetic BZ [35]. Then, to make contact with numerical studies performed in the t-J model [36, 37] and ARPES measurements in underdoped cuprates, Figure 1.2, let us assume that this hole-like pockets are located near the nodal points. In the Figure 4.2, we show the FS structure obtained from the dispersion $\xi_{\boldsymbol{k}}$ in (4.43) with an appropriate chemical potential to account for a doping level of $\delta = 0.050$.

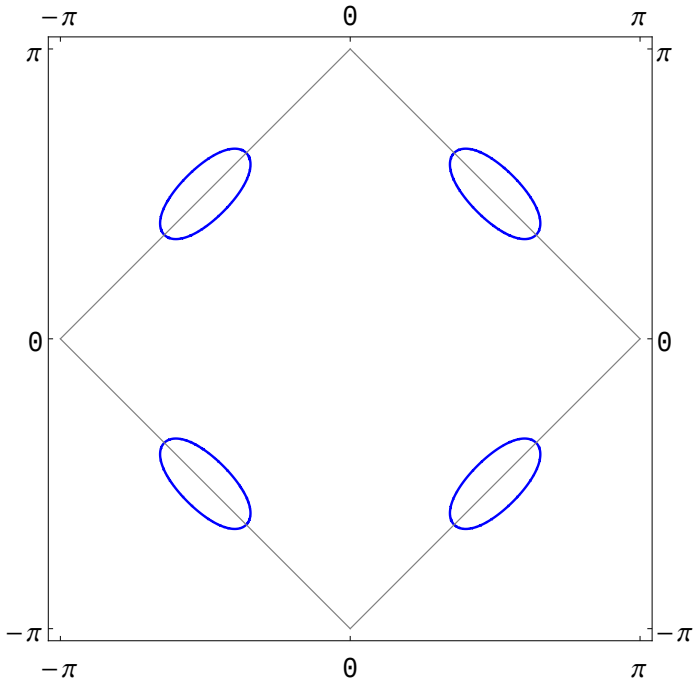

Figure 4.2: Contour plot in blue displaying four elliptical-like Fermi pockets obtained from the vacancy dispersion relation in the presence of an AF background. The chemical potential was adjusted to fix the vacancy density at $\delta = 0.050$. The gray square is the boundary of the magnetic BZ. The bare hopping amplitudes were choosen to be as $t'' = 0.75t' > 0$.

Gauge Coupling and Low Energy

Now let us take into account the gauge field fluctuations around the bare action $S_t^{(0)}[\bar{\eta},\eta]$ in (4.43). Consider for a moment the Wilson loop operator $W(C)$ in (4.17). This time due the staggered nature of the quantization axes $\boldsymbol{\phi}(\boldsymbol{x}_i,\tau) = (-1)^i\boldsymbol{n}(\boldsymbol{x}_i,\tau)$, its expected mean value $\langle W(C)\rangle$ indicates that the flux defined for $\boldsymbol{n}(\boldsymbol{x}_i,\tau)$ threads the intra-sublattice loops in opposite directions for different sublattices.[10] In other words, for

[10]To determine this phase fluctuations is enough just to deal with $\boldsymbol{n}$ since the small ferromagnetic fluctuations are further supressed by $a^2 \to 0$ in the continuum limit.

sites i and j in the same sublattice, the phase fluctuations of the transfer integral T_{ij} (4.12) are given by

$$\arg\Big[\big\langle\boldsymbol{\phi}_i^d\big|\big(1\mp\boldsymbol{\sigma}\cdot\boldsymbol{n}_i\big)\big(1\mp\boldsymbol{\sigma}\cdot\boldsymbol{n}_j\big)\big|\boldsymbol{\phi}_j^d\big\rangle\Big]=\pm\mathcal{A}_{ij}\equiv\pm\int_{\boldsymbol{x}_i}^{\boldsymbol{x}_j}d\boldsymbol{r}\cdot\boldsymbol{\mathcal{A}},\tag{4.44}$$

where we must pick all the upper (lower) signs when i,j belong to the sublattice A (B). In a nutshell, the η-fermions living in different sublattices couple to the emergent gauge field $\mathcal{A}^\mu$ with opposite charges, and, as a result of that, they can attract each other. Later on, we will discuss the possibility that this feature might also be associated with an unconventional superconducting pairing mechanism [38].

To arrive at the low energy description, we just expand the dispersion $\xi_{\boldsymbol{k}}$ around its minima. Since only two of the minima are truly unequivalent due the existence of the reduced AF Brillouin zone, we arbitrarily choose $(\frac{\pi}{2},\frac{\pi}{2})$ and $(-\frac{\pi}{2},\frac{\pi}{2})$. Let us also adopt a more convenient frame which can be obtained after a $\frac{\pi}{4}$-counterclockwise rotation of the original axes. Then, around these minima we find

$$\xi^{(1)}_{\boldsymbol{p}'}=\frac{1}{2m_+}p_x'^2+\frac{1}{2m_-}p_y'^2-\mu\qquad\text{and}\qquad\xi^{(2)}_{\boldsymbol{p}'}=\frac{1}{2m_-}p_x'^2+\frac{1}{2m_+}p_y'^2-\mu,\tag{4.45}$$

where $m_\pm=\frac{1}{4(2t''\pm t')}$ are the effective masses and the primed momentum $\boldsymbol{p}'$ is defined as $\boldsymbol{p}'=\boldsymbol{k}'-(\frac{\pi}{\sqrt{2}},0)$ for the first dispersion, and as $\boldsymbol{p}'=\boldsymbol{k}'-(0,\frac{\pi}{\sqrt{2}})$ for the second. Finally, for small gauge field fluctuations the topology of the FS will not be drastically changed, and we are allowed to make the minimal coupling replacement $p^\mu\to p^\mu\mp\mathcal{A}^\mu$.[11] Hence, the resultant Lagrangian density is

$$\begin{aligned}\mathcal{L}_t[\bar\eta,\eta,\mathcal{A}'_\mu]=\bar\eta_v(\partial_\tau+\sigma_z i\mathcal{A}^0)\eta_v+\bar\eta_1\Big[\tfrac{1}{2m_+}(-i\partial'_x-\sigma_z\mathcal{A}'_x)^2+\tfrac{1}{2m_-}(-i\partial'_y-\sigma_z\mathcal{A}'_y)^2\Big]\eta_1\\+\bar\eta_2\Big[\tfrac{1}{2m_-}(-i\partial'_x-\sigma_z\mathcal{A}'_x)^2+\tfrac{1}{2m_+}(-i\partial'_y-\sigma_z\mathcal{A}'_y)^2\Big]\eta_2,\end{aligned}\tag{4.46}$$

where we have introduced for convenience the two component spinor $\eta_v=\begin{pmatrix}\eta_{v,A}&\eta_{v,B}\end{pmatrix}^T$ notation. Here the index v labels the two unequivalent hole-like pockets (valleys). At last, given that all the primed quantites are defined in the rotated frame, it is a trivial matter to verify the local $U(1)$ gauge invariance of $\mathcal{L}_t[\bar\eta,\eta,\mathcal{A}'_\mu]$.

[11] If needed, the justification of this procedure is available in Appendix D.

Quartic Interaction Term

The charged sector also has the contribution $H_I[\bar{\eta},\eta]$ given in (4.28), which originated from the magnetic term $H_J[\bar{\eta},\eta,\boldsymbol{\phi}]$. After absorbing some innocuous bilinear terms through a redefinition of the chemical potential, $H_I[\bar{\eta},\eta]$ can be written as an appropiate quartic interaction term of the η-fermions, i.e.,

$$H_I[\bar{\eta},\eta] = -J\sum_{\langle ij\rangle}\bar{\eta}_i\bar{\eta}_j\eta_j\eta_i \tag{4.47}$$

We then go to the momentum space. By taking care of the bipartite character of the lattice and its fermions η_A and η_B, we arrive at

$$S_I[\bar{\eta},\eta] = \frac{1}{2\beta N}\sum_{k_1,\ldots,k_4}\bar{\eta}_{k_4 a}\bar{\eta}_{k_3\bar{a}}J_{\boldsymbol{k}_3-\boldsymbol{k}_2}\eta_{k_2\bar{a}}\eta_{k_1 a}\delta_{k_4+k_3-k_2-k_1}, \tag{4.48}$$

where $J_{\boldsymbol{q}} = -2J(\cos q_x + \cos q_y)$ and $\bar{a}$ denotes the opposite sublattice to a.

However, since we are interested in the low energy behavior of $S_I[\bar{\eta},\eta]$ associated with the FS structure presented in the previous section, we are going to separate the full momenta summations into more restricted summations over thin momentum shells around the Fermi pockets. This procedure follows naturally from the inspection of the original bare interaction vertex in the neighbourhood of the s-, t- and u-channels:

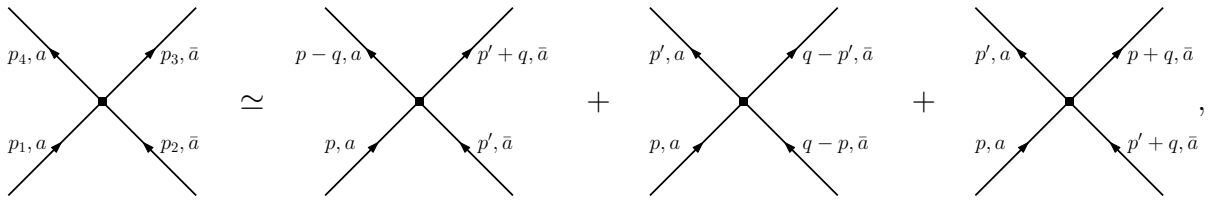

where we assume $|q| \ll |p|, |p'|$. Then, by proceeding to the continuum limit, it is not difficult to arrive at the effective Lagrangian (density) governing the quartic interactions, namely,

$$\mathcal{L}_I[\bar{\eta},\eta] = \tfrac{1}{2}\Big(g_s\bar{\eta}_{va}\bar{\eta}_{v'\bar{a}}\eta_{v'\bar{a}}\eta_{va} + g_t\bar{\eta}_{va}\bar{\eta}_{v\bar{a}}\eta_{v'\bar{a}}\eta_{v'a} + g_u\bar{\eta}_{va}\bar{\eta}_{\bar{v}\bar{a}}\eta_{v\bar{a}}\eta_{\bar{v}a}\Big). \tag{4.49}$$

The g's are coupling constants introduced in analogy with the usual $1+1$ dimensional g-ology notation. In the following we comment briefly on the physical significance of each one of these terms.

To begin with, consider the term arising from the s-channel. Since the η-fermions scatter with a small change in momentum, they will not leave the vicinity of their original pockets, as shown schematically in Figure 4.3. Here we introduce further labels $g_s = \{g_{s1}, g_{s2}\}$ to distinguish processes with $v' = v$ and $v' = \bar{v}$. In any case, at this bare level the strength of the coupling can be estimated to be $g_s \sim J_{\boldsymbol{q}=0} = -4J$.

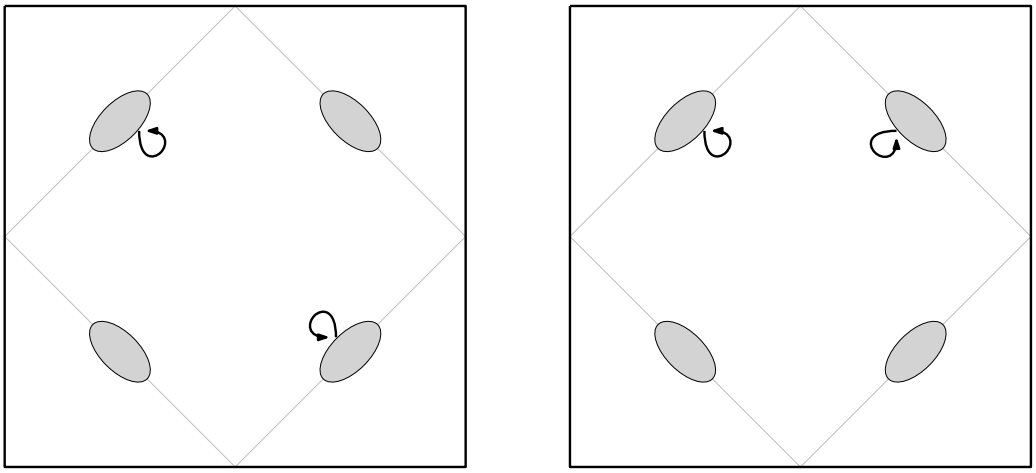

Figure 4.3: Schematic examples of low energy processes generated by the s-channel.

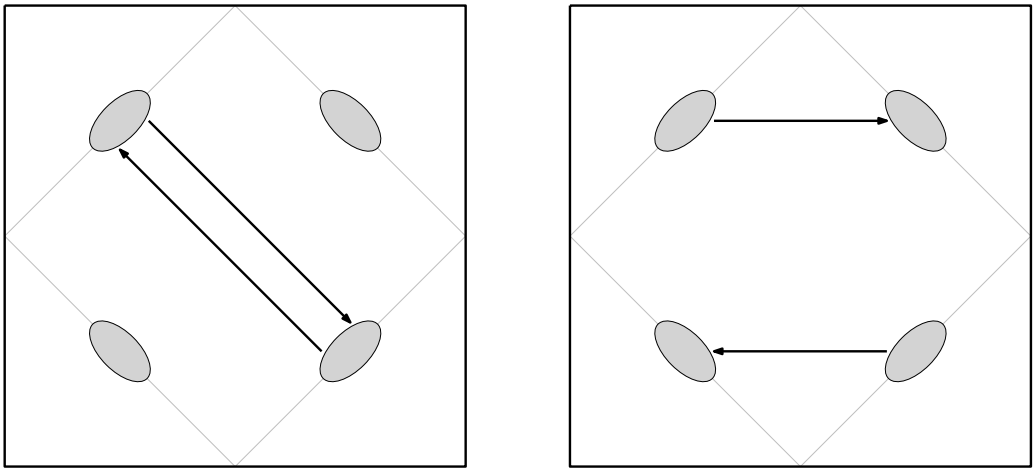

Figure 4.4: Schematic examples of low energy processes generated by the t-channel.

Moving forward, we now consider the t-channel term. At the small $|q|$ regime, it can be related to scattering processes which start and end at opposite regions of the BZ, as depicted in Figure 4.4. For instance, if $v' = v$, the interaction term will map opposite sides of the same pocket which could lead to a conventional BCS instability, as can be seen on the left panel of Figure 4.4. However, since the coupling $g_{t1} \sim J_{(\pi,\pi)} = 4J$ appears to be positive, the possibility of such a pair formation may be difficult to accomplish in this case.

At last, there is the u-channel term which can be easily related to inter pocket processes as indicated in Figure 4.5. There we can see that this channel might be responsible for the emergence of DWs with modulation vectors aligned horizontally/vertically, as it is indeed verified experimentally. However, if we make a direct estimate for the coupling constant, it turns out that it vanishes $g_u \sim J_{(\pi,0)} = J_{(0,\pi)} = 0$. This indicates that this sort of process shall only be activated after reaching a critical density of vacancies δ_{DW}. That is, when there will be enough fermions located away from its pocket center. For example, to get a rough estimate, let us take a configuration in which the minimal distance connecting unequivalent pockets is $\frac{2\pi}{3}$. Then, the coupling may be of the order $g_{t2} \sim J_{(\frac{2\pi}{3},0)} = J_{(0,\frac{2\pi}{3})} = -J$ and, as a result of that, only the fermions at the immediate vicinity of the pockets will be coupled to each other.

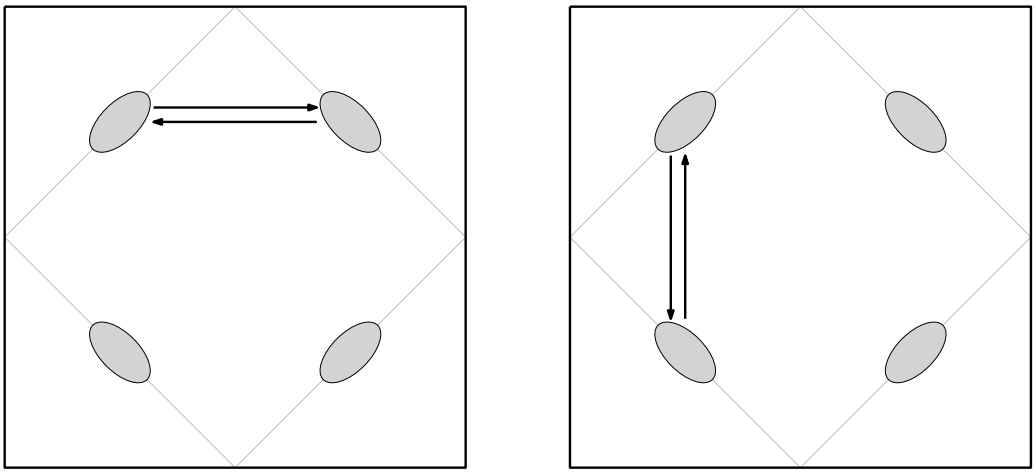

Figure 4.5: Schematic examples of low energy processes generated by the u-channel.

4.2.3 Effective Lagrangian for an Underdoped AF

In the previous section, we have concluded the last step of our approximate scheme. By collecting all our results together, we arrive at the sought effective model for the lightly doped AF, $\mathcal{L}[\bar{\eta},\eta,\mathcal{A}_\mu] = \mathcal{L}_t[\bar{\eta},\eta,\mathcal{A}_\mu] + \mathcal{L}_I[\bar{\eta},\eta] + \mathcal{L}_{\mathrm{spin}}[\mathcal{A}_\mu]$ where each one of these terms were defined in (4.46), (4.49) and (4.41), respectively. In a more explicit form, this Lagrangian reads

$$\begin{aligned}\mathcal{L}[\bar{\eta},\eta,\mathcal{A}_\mu] = \bar{\eta}_v(\partial_\tau + \sigma_z i\mathcal{A}^0)\eta_v + \bar{\eta}_1\Big[\tfrac{1}{2m_+}(-i\partial_x - \sigma_z\mathcal{A}_x)^2 + \tfrac{1}{2m_-}(-i\partial_y - \sigma_z\mathcal{A}_y)^2\Big]\eta_1 \\ + \bar{\eta}_2\Big[\tfrac{1}{2m_-}(-i\partial_x - \sigma_z\mathcal{A}_x)^2 + \tfrac{1}{2m_+}(-i\partial_y - \sigma_z\mathcal{A}_y)^2\Big]\eta_2 + \frac{1}{4\kappa^2}(\mathcal{F}_{\mu\nu})^2 \\ + g\text{-quartic interaction terms.} \qquad (4.50)\end{aligned}$$

Here we simply omit the primes in the spatial elements because $\mathcal{L}_I[\bar{\eta},\eta]$ and $\mathcal{L}_{\rm spin}[\mathcal{A}_\mu]$ are both invariant under rotations, and all these terms are now defined in the same $\frac{\pi}{4}$-rotated frame.

We stress that similar descriptions for this problem were proposed much earlier by Shankar [39] and Lee [35]. Despite the presence of the quartic interaction terms, in comparison to the theory in [39], the present proposal also features fewer degrees of freedom. This happens because, differently from there, the Lagrangian (4.50) does not contain explicitly the $\boldsymbol{n} \in S^2$ field which has necessarily two degrees of freedom. In contrast with that, after recasting this field in the CP^1 representation, we integrated out the z-bosons to arrive at a description only in terms of the emergent gauge field $\mathcal{A}^\mu$. At first sight, it may seem that $\mathcal{A}^\mu$ introduces three degrees of freedom, each one them associated with one of its components. However since $\mathcal{A}^0$ has no kinetical term in the Maxwell Lagrangian, it is not dynamical. Moreover, by gauge fixing (e.g., $\nabla \cdot \boldsymbol{\mathcal{A}} = 0$) one is always able to get rid of one extra degree of freedom. It turns out, that for the (2+1) spacetime dimensions that we are working with, there is only one physical degree of freedom associated to $\mathcal{A}^\mu$.[12] On the other hand, the Lee's description is closer related to ours. So that, besides the quartic interaction terms, it just differs in the bare FS structure which is composed of only one hole-like pocket located in the center of the BZ.

Physical Observables, Density Waves and Pairing Mechanism

The physical Green's function of the present effective theory is (up to some numerical factor) given by

$$\langle \tilde{c}_i^\dagger \tilde{c}_j \rangle \sim \langle \eta_i e^{i\mathcal{A}_{ij}} \bar{\eta}_j \rangle, \tag{4.51}$$

as one can readily verify by using directly the formula (2.11) for $\tilde{c}_{i\sigma}^\dagger$. This does not just reveals the hole-like character of the η-fermions, but also tells us that well-defined physical observables must be gauge invariant quantities with respect to the emergent gauge field $\mathcal{A}^\mu$.

To ilustrate this point, consider the following mean-field (MF) Hamiltonian obtained from the combination of $L_t[\bar{\eta},\eta,\boldsymbol{\phi}]$ in (4.16) and $H_I[\bar{\eta},\eta]$ in (4.47). If we decouple the

[12] The same line of reasoning leads to the two physical polarization states of the photon in $(3+1)$ spacetime dimensions.

quartic interaction and neglect fluctuations, we find

$$H_{\text{MF-DW}}[\bar{\eta},\eta] = \sum_{ij}\left(\tilde{t}_{ij}\bar{\eta}_i e^{i\mathcal{A}_{ij}}\eta_j + \text{h.c.}\right) - \sum_{\langle ij\rangle}\left(\chi_{ij}\bar{\eta}_i e^{i\mathcal{A}_{ij}}\eta_j + \text{h.c.}\right) \tag{4.52}$$

where $\chi_{ij} = -J\langle\bar{\eta}_j e^{i\mathcal{A}_{ji}}\eta_i\rangle$ is a gauge invariant bond DW MF parameter. In Figure 4.6, we plot the spectral function associated with the Hamiltonian $H_{\text{MF-DW}}[\bar{\eta},\eta]$ for a Néel background configuration with zero total flux, assuming a d-wave DW order parameter $\chi_{\boldsymbol{Q}}(\boldsymbol{k}) = \chi_0(\cos k_x - \cos k_y)$. The bidirectional modulation vectors are respectively $\boldsymbol{Q}_x = (\frac{2\pi}{3}, 0)$ and $\boldsymbol{Q}_y = (0, \frac{2\pi}{3})$ of three unit-cell periodicity in the x and y directions. To get a rough estimation we have set $\chi_0 = J\delta$ with $J = 2t'$.

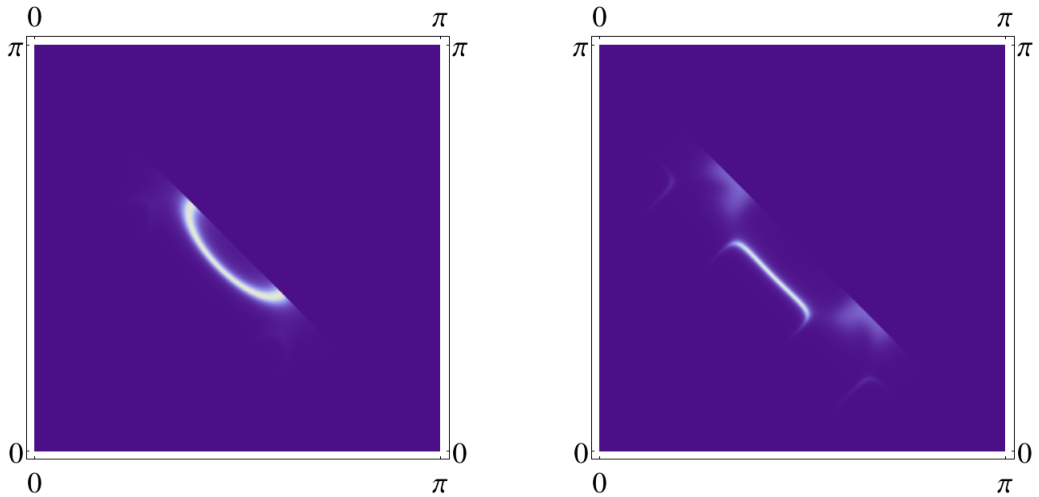

Figure 4.6: Spectral function at the Fermi level within the first quadrant of the AF BZ for bidirectional DW with modulation vectors $\boldsymbol{Q}_x = (\frac{2\pi}{3}, 0)$ and $\boldsymbol{Q}_y = (0, \frac{2\pi}{3})$. In parts (a) and (b), we have $\delta = 0.030$ and $\delta = 0.070$, respectively. The spectral function was calculated numerically with a Lorentzian broadening of $\epsilon = 0.02t'$.

The result of Figure 4.6 reinforces our earlier discussions on the effective coupling parameter g_u. As it can be seen in the numerical results, at very small dopings there is no nesting between the different patches of the Fermi pockets along the BZ. The DW gap only opens after reaching a critical density which allows the nesting of the modulation vector near the periphery of the pockets.

Finally, let us briefly discuss here the pairing mechanism proposed by Wiegmann [38]. Within the Lagrangian (4.50), the exchange of photons of the emergent gauge field $\mathcal{A}^\mu$ may lead the system towards an instability with respect the condensation of the gauge

invariant pair propagator

$$\langle \bar{\eta}_A(x)\bar{\eta}_B(x)\eta_B(0)\eta_A(0)\rangle \to |\Delta|^2. \tag{4.53}$$

However since the η-fermions are equally charged with respect electromagnetic (EM) field, this phase transition breaks down the EM $U(1)$ gauge symmetry and, therefore, leads to superconductivity.[13]

[13]This possibility will be further explored in the near future.

Chapter 5

Conclusions and Perspectives

In this work we have explored the doped carrier formulation to present an effective model (2.28) that provides an alternative way to deal with the underdoped regime of the canonical t-J model. The faithfulness of such description was then readily verified through two simple tests. While one of them examined the existence of strong correlations, the other studied the role of the representation adopted for the hopping term. From it was also possible to extract deeper insights into the role of the introduced constraint operator. It would also be interesting to inspect the Hamiltonian (2.28) using more powerful numerical methods (like cluster perturbation theory) in order to explore whether or not the proposed model can provide an amenable starting point there.

The construction of a path integral representation for the t-J quantum partition function from spin-dopon variables was also object of discussion in our work. In this matter, we were able to reproduce the $su(2|1)$ formulation, and to attempt a different approach based on the properties of the constraint operator. From the latter approach, we extracted an effective description (4.22) after resorting to an approximation scheme. In spite of our severe approximations, this approach was able to recover the exact ground-state energy result for the $U = \infty$ Hubbard model in one spatial dimension. Then, in order to make contact with high-T_c cuprates, we derived from (4.22) a continuum field theory in $(2 + 1)$ spacetime dimensions. The resulting field theory (4.50) describes interacting spinless fermions coupled to a dynamical $U(1)$ gauge field. It also features several striking properties which seems to be at least qualitatively in agreement with experiments. Apart from an unconventional mechanism for superconductivity, it is also able to describe diverse low energy scattering processes which can be associated with different physical phenomena

such as the DWs, which are observed in experiments. This approach could be put into further test, if one computes the associated transport properties at zero and finite temperature to compare the results with the experimental data. Another exciting possiblity is the development of exactly soluble toy models for the $su(2|1)$ path integral formalism. In particular, if successful, this would no doubt be extremely helpful to shed more light into the physics of the t-J model.

Finally, to conclude, let us highlight the possible connection between the t-J physics with other well known strongly correlated system. Apart from the already mentioned connection with the heavy-fermions compounds, more recently, the large U Hubbard model has been studied within the framework of optical lattice experiments. In particular, there are now routes for the realization of fractional quantum Hall effect (FQHE) in those systems [40]. In view of that, it is worthwhile to notice that the model (4.22) can also account for P, T symmetry breaking ground-states characterized by values of the flux $\Phi \neq 0, \pi$, as seen from (4.20). This might enlarge the scope of possible applications of the effective model presented here.

Appendix A

The $su(2|1)$ Coherent-State Manifold

The on-site Hilbert space of the t-J model is spanned by the three states $\{|a\rangle\} = \{|0\rangle, |\uparrow\rangle, |\downarrow\rangle\}$ as was given on (1.3). Then, it should be obvious that any physical sensible operator within this Hilbert space can be translated in terms of the projection operators $X^{ab} = |a\rangle\langle b|$ popularly known as Hubbard operators. The key point here is that the fermionic Hubbard operators $X^{0\sigma} = (X^{\sigma 0})^\dagger$ along with the bosonic ones $X^{\sigma\sigma'}$ and X^{00}, are closed under commutation/anticommutation relations of the superalgebra $su(2|1)$:

$$\{X_i^{ab}, X_j^{cd}\}_\mp = \delta_{ij}(X_i^{ad}\delta^{bc} \mp X_i^{cb}\delta^{ad}) \tag{A.1}$$

where i, j are lattice site labels and $(+)$ should only be used in the case when both operators are fermionic [38]. While we do not intent to go into deeper details on this subject (and refer instead to the works [26, 41] and references therein), we shall present some basic tools necessary to work with it.

To put it simply, the $su(2|1)$ superalgebra can be thought of as the simplest possible extension of the conventional spin $su(2)$ algebra to incorporate fermionic degrees of freedom. Its bosonic sector consists of three bosonic superspin operators,

$$Q^+ = X^{\uparrow\downarrow}, \qquad Q^- = X^{\downarrow\uparrow} \qquad \text{and} \qquad Q^z = \tfrac{1}{2}(X^{\uparrow\uparrow} - X^{\downarrow\downarrow}) \tag{A.2}$$

closed into $su(2)$, along with the vacancy number operator X^{00} that generates a $u(1)$ factor of the maximal even subalgebra $su(2) \times u(1)$ of $su(2|1)$. On the other hand, the fermionic sector is constructed out of the remaining four operators that transform in a spinor representation of $su(2)$.

The normalizable coherent-states associated with the lowest irreducible representation of the $su(2|1)$ superalgebra spanned by the Hubbard operators reads

$$|z,\xi\rangle = \frac{\exp\left(zX^{\downarrow\uparrow} + \xi X^{0\uparrow}\right)}{\sqrt{1+\bar{z}z+\bar{\xi}\xi}}\,|\uparrow\rangle = \frac{1}{\sqrt{1+\bar{z}z+\bar{\xi}\xi}}(|\uparrow\rangle + z\,|\downarrow\rangle + \xi\,|0\rangle) \tag{A.3}$$

where a complex even Grassmann parameter z and an odd complex Grasmmann parameter ξ are the inhomogeneuos (proper) coordinates of a point on a supersphere $(z,\xi) \in S^{2|2} \simeq CP^{1|1} = SU(2|1)/U(1|1)$.[1] Here $CP^{1|1}$ stands for a complex projective superspace with a complex dimension $(1,1)$. It can be thought of as a minimal superextension of an ordinary projective space CP^1 homeomorphic to a two-sphere, $CP^1 \simeq S^2$. By using the homogeneous coordinates (z^1, z^2, θ) on the supersphere, so that $z = z^1/z^2$ and $\xi = \theta/z^2$ with $z^2 \neq 0$. The coset $CP^{1|1}$ manifold is then defined by the equation

$$|z^1|^2 + |z^2|^2 + \bar{\theta}\theta = 1. \tag{A.4}$$

It is worthwhile to notice that at $\xi = 0$, the $su(2|1)$ coherent-state (A.3) reduces to the ordinary spin $su(2)$ coherent-state representation as expected

$$|z,\xi=0\rangle = \frac{1}{\sqrt{1+|z|^2}}\left(\,|\uparrow\rangle + z\,|\downarrow\rangle\,\right) \tag{A.5}$$

where the complex number z is a stereographic coordinate of a point on an ordinary sphere, $z \in S^2 \simeq SU(2)/U(1)$.

Another key ingredient in the representation theory of the $su(2|1)$ algebra is the resolution of identity which is simply given by

$$I = \int d\mu_{su(2|1)}\,|z,\xi\rangle\,\langle z,\xi| \tag{A.6}$$

provided that the integration measure takes the form

$$d\mu_{su(2|1)} = \frac{d\bar{z}dzd\bar{\xi}d\xi}{2\pi i(1+\bar{z}z+\bar{\xi}\xi)}. \tag{A.7}$$

[1]The odd Grassmann parameter ξ is needed to make the product $\xi X^{0\uparrow}$ represent a bosonic quantity as required.

Partition Function: $su(2|1)$ Path Integral Representation

Evaluating the quantum partition function for a given Hamiltonian H in the $\{|z,\xi\rangle\}$ basis results in a $su(2|1)$ path integral representation

$$\mathcal{Z} = \operatorname{tr} e^{-\beta H} = \int d\mu_{su(2|1)} \, \langle z,\xi| \, e^{-\beta H} \, |z,-\xi\rangle \equiv \int \mathcal{D}\mu_{su(2|1)} e^{-S[\bar{z},z,\bar{\xi},\xi]}, \tag{A.8}$$

where the action of the theory is

$$S[\bar{z},z,\bar{\xi},\xi] = \int_0^\beta d\tau \Big[-\frac{1}{2}\Big(\frac{\dot{\bar{z}}z - \bar{z}\dot{z} + \dot{\bar{\xi}}\xi - \bar{\xi}\dot{\xi}}{1+\bar{z}z+\bar{\xi}\xi}\Big) + H(\bar{z},z,\bar{\xi},\xi)\Big] \tag{A.9}$$

and $\mathcal{D}\mu_{su(2|1)}$ stands for an infinite pointwise product of $su(2|1)$ invariant measures (A.7). To explicitly evaluate $H(\bar{z},z,\bar{\xi},\xi)$ one needs the so called coherent-state symbols defined as $\langle X\rangle = \langle z,\xi| \, X \, |z,\xi\rangle$. These are found to be

$$\begin{aligned} &\langle X^{00}\rangle = w\bar{\xi}\xi, \qquad \langle Q^z\rangle = \tfrac{1}{2}w(1-|z|^2), \qquad \langle Q^+\rangle = wz, \qquad \langle Q^-\rangle = w\bar{z}, \\ &\langle X^{0\downarrow}\rangle = wz\bar{\xi}, \qquad \langle X^{0\uparrow}\rangle = w\bar{\xi}, \qquad \langle X^{\downarrow 0}\rangle = w\bar{z}\xi \qquad \text{and} \qquad \langle X^{0\uparrow}\rangle = w\xi \end{aligned} \tag{A.10}$$

where we have introduced $w = (1+\bar{z}z+\bar{\xi}\xi)^{-1}$ to ease the notation.

However, as mentioned in the main text, the emergent integration measure in this representation makes any further progress quite difficult. As a result, no nontrivial computations are available so far making use of this approach.

Appendix B

Effective Action for the Spin Sector

To obtain the long wavelength limit of the action $S_{\text{spin}}[\boldsymbol{\phi}]$ on (4.31), we will begin by evaluating the expression $(\boldsymbol{\phi}_i + \boldsymbol{\phi}_j)^2$ in the continuum limit. Let us consider a first neighbor site to $\boldsymbol{x}_i$ labelled by the vector $\boldsymbol{x}_j = \boldsymbol{x}_i + a\hat{\boldsymbol{x}}$. Taking into consideration that $\boldsymbol{n}(\boldsymbol{x}, \tau)$ is a smooth field configuration, we may write the spin field at the j site as

$$\boldsymbol{\phi}(\boldsymbol{x}_j, \tau) = -(-1)^i \big[\boldsymbol{n}(\boldsymbol{x}_i, \tau) + a\partial_x \boldsymbol{n}(\boldsymbol{x}_i, \tau)\big] + a^2 \boldsymbol{l}(\boldsymbol{x}_i, \tau) + \mathcal{O}(a^4). \tag{B.1}$$

Together with (4.27), this gives us that

$$\begin{aligned}\big(\boldsymbol{\phi}_i + \boldsymbol{\phi}_j\big)^2 &= \Big[-(-1)^i a\partial_x \boldsymbol{n}(\boldsymbol{x}_i, \tau) + 2a^2 \boldsymbol{l}(\boldsymbol{x}_i, \tau)\Big]^2 \\ &= a^2 |\partial_x \boldsymbol{n}(\boldsymbol{x}_i, \tau)|^2 - 4a^3 (-1)^i \partial_x \boldsymbol{n}(\boldsymbol{x}_i, \tau) \cdot \boldsymbol{l}(\boldsymbol{x}_i, \tau) + 4a^4 |\boldsymbol{l}(\boldsymbol{x}_i, \tau)|^2. \end{aligned} \tag{B.2}$$

However, note that the term proportional to $(-1)^i$ will be cancelled out when we take into account the contributions coming from the link connecting the opposite nearest neighbor site, $\boldsymbol{x}_j = \boldsymbol{x}_i - a\hat{\boldsymbol{x}}$. Collecting the resulting contributions of the other two terms along the $\hat{\boldsymbol{y}}$ direction and substituing them on the formula (4.30) for $H_{\text{spin}}[\boldsymbol{\phi}]$, one eventually arrives at

$$\begin{aligned} H_{\text{spin}}[\boldsymbol{n}, \boldsymbol{l}] &= \frac{s^2 \tilde{J} a^2}{2} \sum_i \Big(|\nabla \boldsymbol{n}(\boldsymbol{x}_i, \tau)|^2 + 8a^2 |\boldsymbol{l}(\boldsymbol{x}_i, \tau)|^2 \Big) \\ &\equiv \frac{\tilde{J} s^2}{2} \int d^2x \Big(|\nabla \boldsymbol{n}(\boldsymbol{x}, \tau)|^2 + 8a^2 |\boldsymbol{l}(\boldsymbol{x}, \tau)|^2 \Big). \end{aligned} \tag{B.3}$$

On the other hand, we also need to rewrite the topological action $isS_{\rm WZ}[\boldsymbol{\phi}]$ in terms of the new smooth fields $\boldsymbol{n}$ and $\boldsymbol{l}$. Using (4.4) for the Wess-Zumino term, let us consider the expression

$$\begin{aligned}\boldsymbol{\phi}(\tau,\upsilon)\cdot\big[\partial_\tau\boldsymbol{\phi}(\tau,\upsilon)\times\partial_\upsilon\boldsymbol{\phi}(\tau,\upsilon)\big] &= \\ &= (-1)^i\boldsymbol{n}\cdot(\partial_\tau\boldsymbol{n}\times\partial_\upsilon\boldsymbol{n}) + a^2\boldsymbol{n}\cdot(\partial_\tau\boldsymbol{n}\times\partial_\upsilon\boldsymbol{l}) + a^2\boldsymbol{n}\cdot(\partial_\tau\boldsymbol{l}\times\partial_\upsilon\boldsymbol{n}) \\ &\quad + a^2\boldsymbol{l}\cdot(\partial_\tau\boldsymbol{n}\times\partial_\upsilon\boldsymbol{n}) + \mathcal{O}(a^4),\end{aligned} \tag{B.4}$$

keeping only the leading order terms. Given that $\boldsymbol{l}$, $\partial_\tau\boldsymbol{n}$ and $\partial_\upsilon\boldsymbol{n}$ are coplanar vectors, the last relevant term on the right-hand side vanishes. Moreover, one should note that the first term is cancelled out for smooth continuous field configurations in two spatial dimensions.[1] Therefore, we are left with only two terms of (B.4) that we can rewrite in a simpler form. For example, one of them can be cast as

$$\boldsymbol{n}\cdot(\partial_\tau\boldsymbol{n}\times\partial_\upsilon\boldsymbol{l}) = \partial_\upsilon\big[\boldsymbol{n}\cdot(\partial_\tau\boldsymbol{n}\times\boldsymbol{l})\big] \tag{B.5}$$

since $\partial_\upsilon\boldsymbol{n}\cdot(\partial_\tau\boldsymbol{n}\times\boldsymbol{l}) = \boldsymbol{n}\cdot(\partial_\upsilon\partial_\tau\boldsymbol{n}\times\boldsymbol{l}) = 0$. Obviously, a similar relation holds for $\boldsymbol{n}\cdot(\partial_\tau\boldsymbol{l}\times\partial_\upsilon\boldsymbol{n})$. Hence, the Wess-Zumino term (4.4) will read

$$S_{\rm WZ}[\boldsymbol{n},\boldsymbol{l}] = a^2\sum_i\int_0^\beta d\tau\int_0^1 d\upsilon\,\Big\{\partial_\upsilon\big[\boldsymbol{n}_i\cdot(\partial_\tau\boldsymbol{n}_i\times\boldsymbol{l}_i)\big] + \partial_\tau\big[\boldsymbol{n}_i\cdot(\boldsymbol{l}_i\times\partial_\upsilon\boldsymbol{n}_i)\big]\Big\}. \tag{B.6}$$

Performing the integrals in the expression above and using the boundary conditions provided in (4.5), we are eventually led to the result

$$S_{\rm WZ}[\boldsymbol{n},\boldsymbol{l}] = -a^2\sum_i\int_0^\beta d\tau\;\boldsymbol{n}_i\cdot(\partial_\tau\boldsymbol{n}_i\times\boldsymbol{l}_i). \tag{B.7}$$

Thus, in the continuum limit, the sought topological term is given by

$$isS_{\rm WZ}[\boldsymbol{n},\boldsymbol{l}] = -is\int d^3x\;\boldsymbol{l}\cdot(\boldsymbol{n}\times\partial_\tau\boldsymbol{n}). \tag{B.8}$$

[1] This is a subtle step since in one spatial dimension the term $(-1)^i\boldsymbol{n}\cdot(\partial_\tau\boldsymbol{n}\times\partial_\upsilon\boldsymbol{n})$ is responsible for the emergence of a Hopf term in the effective Lagrangian. The reason for the cancellation of this term in two spatial dimensions can be understood naively by the nature of the Néel state. If we take each row separately, each one of them will give rise to a one dimensional Hopf term. However neighbouring rows are staggered in a opposite way. The net result is an effective cancellation for each pair of rows.

Returning to the entire action of the spin sector (4.31), we have

$$S_{\text{spin}}[\boldsymbol{n},\boldsymbol{l}] = \frac{1}{2}\int d^3x\Big[\tilde{J}s^2|\nabla\boldsymbol{n}|^2 + 8\tilde{J}s^2a^2|\boldsymbol{l}|^2 - 2is\boldsymbol{l}\cdot(\boldsymbol{n}\times\partial_\tau\boldsymbol{n})\Big]. \tag{B.9}$$

Since the ferromagnetic fluctuations are always suppressed by a factor of a^2, we can neglect further contributions coming from $L_t[\bar{\eta},\eta,\boldsymbol{\phi}]$ which are already small due to the low density of vacancies, $\delta \ll 1$. We then may perform the trivial integration over the ferromagnetic fluctuation $\boldsymbol{l}$ to arrive at

$$S_{\text{spin}}[\boldsymbol{n}] = \frac{1}{2}\int d^3x\left[\tilde{J}s^2|\nabla\boldsymbol{n}|^2 + \frac{1}{8\tilde{J}a^2}(\boldsymbol{n}\times\partial_\tau\boldsymbol{n})^2\right]. \tag{B.10}$$

But since $|\boldsymbol{n}|^2 = 1$ and $\boldsymbol{n}\perp\partial_\tau\boldsymbol{n}$, we have $(\boldsymbol{n}\times\partial_\tau\boldsymbol{n})^2 = (\partial_\tau\boldsymbol{n})^2$. Making this substitution results in the $O(3)$ NLσM presented in the main text,

$$S_{\text{spin}}[\boldsymbol{n}] = \frac{1}{2g}\int d^3x\left(c_s^{-1}|\partial_\tau\boldsymbol{n}|^2 + c_s|\nabla\boldsymbol{n}|^2\right), \tag{B.11}$$

where $g = 2\sqrt{2}a/s$ and $c_s = 2\sqrt{2}\tilde{J}sa$ are respectively an effective coupling constant and the spin-wave velocity.

The Role of Quantum Fluctuations

In this section, we will take into account the effects of fluctuations to determine in a mean-field analysis the possible different phases associated with the action (B.11). After the inclusion of a Lagrange multiplier field $\lambda(x)$ to implement the condition $|\boldsymbol{n}|^2 = 1$, the partition function will read

$$\mathcal{Z}_{\text{AF}} = \int\mathcal{D}\boldsymbol{n}\mathcal{D}\lambda\ \exp\left\{-\frac{1}{2g}\int d^3x\Big[(\partial_\mu\boldsymbol{n})^2 + i\lambda(\boldsymbol{n}^2-1)\Big]\right\}. \tag{B.12}$$

Henceforth, we are setting $c_s = 1$ for convenience. The inclusion of these factors in the final formulas can also be assured by dimensional analysis. Integrating out the $\boldsymbol{n}$ field, we arrive at an effective theory for the λ field,

$$\mathcal{Z}_{\text{AF}} = \int\mathcal{D}\lambda\ \exp\left\{\frac{1}{2g}\int d^3x\ i\lambda(x) - \frac{\mathcal{N}}{2}\log\det\big[g^{-1}(-\partial^2+i\lambda)\big]\right\} \tag{B.13}$$

where $\mathcal{N} = 3$ is the number of components of the $\boldsymbol{n}$ field. Here we see that by taking $\mathcal{N}$ to be large, since it enters as a prefactor on the effective action, the saddle-point approximation will be applicable. Indeed the mean-field solution can be regarded as exact at the limit $\mathcal{N} \to \infty$ [42]. For a finite $\mathcal{N}$, one may still perform a $1/\mathcal{N}$ expansion as carried out by Polyakov [17] for the $(1+1)$ dimensional case.

Either way, the stationary phase condition for our $\mathcal{N} = 3$ effective action will be

$$\left\langle \frac{\delta S_{\text{eff}}}{\delta \lambda} \right\rangle = \frac{1}{2g} - \frac{\mathcal{N}}{2} \operatorname{tr} \frac{i}{-\partial^2 + i\langle\lambda\rangle} = 0, \tag{B.14}$$

which by setting $i\langle\lambda\rangle = m^2$ for notational convenience, tell us that

$$1 = \frac{\mathcal{N}g}{\beta} \sum_{i\omega_n} \int \frac{d^2k}{(2\pi)^2} \frac{1}{\omega_n^2 + \boldsymbol{k}^2 + m^2}, \tag{B.15}$$

where ω_n are bosonic Matsubara frequencies. Inspecting (B.15), it is not difficult to verify that the integral is in fact UV divergent. We then introduce a heavy Pauli-Villars regulator field, such that the equation now reads

$$1 = \frac{\mathcal{N}g}{\beta} \sum_{i\omega_n} \int \frac{d^2k}{(2\pi)^2} \left(\frac{1}{\omega_n^2 + \boldsymbol{k}^2 + m^2} - \frac{1}{\omega_n^2 + \boldsymbol{k}^2 + \Lambda^2} \right). \tag{B.16}$$

Hence, to find a formula for m, we need to perform the Matsubara sum and the momentum integration. After evaluating the sum over frequencies, we eventually get

$$1 = \mathcal{N}g \int \frac{d^2k}{(2\pi)^2} \left[\frac{\coth\left(\frac{\beta}{2}\sqrt{\boldsymbol{k}^2 + m^2}\right)}{2\sqrt{\boldsymbol{k}^2 + m^2}} - \frac{\coth\left(\frac{\beta}{2}\sqrt{\boldsymbol{k}^2 + \Lambda^2}\right)}{2\sqrt{\boldsymbol{k}^2 + \Lambda^2}} \right]. \tag{B.17}$$

We then readily compute the momentum integral left, to arrive at

$$1 = \frac{\mathcal{N}g}{2\pi\beta} \log \left[\frac{\sinh\left(\frac{1}{2}\beta\Lambda\right)}{\sinh\left(\frac{1}{2}\beta m\right)} \right]. \tag{B.18}$$

Therefore, by inverting the equation above, we find

$$m = \frac{2}{\beta} \sinh^{-1} \left[e^{-\frac{2\pi\beta}{\mathcal{N}g}} \sinh\left(\tfrac{\beta\Lambda}{2}\right) \right]. \tag{B.19}$$

At the low temperature limit, one should notice that the solution (B.19) behaves very

differently depending wheter the coupling constant g is larger or smaller than

$$g_c = \frac{4\pi}{\mathcal{N}\Lambda}. \tag{B.20}$$

Let us first consider the case when $g < g_c$. For large values of β, the argument expression inside the $\sinh^{-1}$ is small and, as a result, the mass must be of the same magnitude, i.e.,

$$m \simeq \beta^{-1} \exp\left[-\frac{2\pi\beta}{\mathcal{N}}\left(\frac{1}{g} - \frac{1}{g_c}\right)\right]. \tag{B.21}$$

Although at $T > 0$, the system has an exponentially small non vanishing mass. Precisely at $T = 0$, we will have $m = 0$ and the correlation legth $\xi_s \sim m^{-1}$ diverges as a signature of the long range AF order.

We now turn to the case when $g > g_c$. This time the argument of the function $\sinh^{-1}$ is large at this low temperature regime. Then, performing an expansion, we find

$$m \simeq m_o + 2\beta^{-1} e^{-\beta m_o}, \tag{B.22}$$

where $m_o = \frac{4\pi}{\mathcal{N}}(g_c^{-1} - g^{-1})$. That is, even at $T = 0$, there is a finite mass gap on the spectrum generated by quantum fluctuations. Thus, the system will have a finite correlation length ξ_s, which is characteristic of the short range AF order.

Appendix C

The Gauge Effective Action

After the integration of the z-bosons, we arrived at (4.38) which, in its turn, can be rewritten as

$$S_{\text{eff}}[\mathcal{A}_\mu] = \text{const.} + 2\,\text{tr}\log\Big[2g^{-1}\Big(1 - \frac{\mathcal{A}_\mu i\overset{\leftrightarrow}{\partial}_\mu}{-\partial^2+m^2} + \frac{\mathcal{A}_\mu\mathcal{A}^\mu}{-\partial^2+m^2}\Big)\Big], \tag{C.1}$$

where the constant is related to the free contribution of the z fields. In the saddle-point approximation spirit, we expand the expression (C.1) around the configuration $\langle\mathcal{A}^\mu\rangle = 0$.[1] Then, the first non-vanishing contributions come from the quadratic terms

$$S^{(2)}_{\text{eff}}[\mathcal{A}_\mu] = 4g^{-1}\,\text{tr}\,\frac{\mathcal{A}_\mu\mathcal{A}^\mu}{-\partial^2+m^2} - 2g^{-1}\,\text{tr}\left(\frac{\mathcal{A}_\mu i\overset{\leftrightarrow}{\partial}_\mu}{-\partial^2+m^2}\right)^2. \tag{C.2}$$

This means that, by neglecting higher order terms, the effective action reads

$$S_{\text{eff}}[\mathcal{A}_\mu] \equiv \frac{1}{2}\int\frac{d^3q}{(2\pi)^3}\mathcal{A}_\mu(q)\Pi^{\mu\nu}(q)\mathcal{A}_\nu(-q), \tag{C.3}$$

where $\Pi^{\mu\nu}(q)$ is the 1PI z-boson current-current correlation function given by the vacuum polarization diagrams:

$\Pi^{\mu\nu}(q) =$ 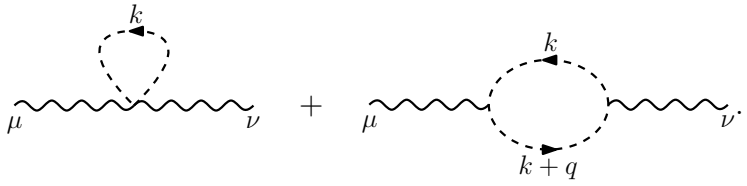

. (C.4)

[1] Keep in mind that this is the same regime applied on the charge sector to arrive at the effective Lagrangian $\mathcal{L}_t[\bar\eta,\eta,\mathcal{A}'_\mu]$ in equation (4.46).

The first diagram is simply

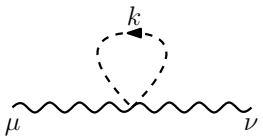

$$= 4g^{-1}\int \frac{d^3k}{(2\pi)^3}\frac{2\delta^{\mu\nu}}{k^2+m^2} \tag{C.5}$$

while the second contribution gives

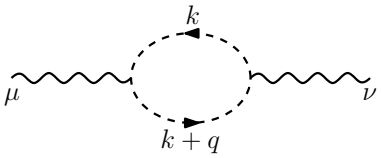

$$= -4g^{-1}\int \frac{d^3k}{(2\pi)^3}\frac{(2k+q)^\mu(2k+q)^\nu}{[(k+q)^2+m^2](k^2+m^2)}. \tag{C.6}$$

Adding both expressions, we get that

$$\Pi^{\mu\nu}(q) = 4g^{-1}\int \frac{d^3k}{(2\pi)^3}\frac{2\delta^{\mu\nu}[(k+q)^2+m^2]-(2k+q)^\mu(2k+q)^\nu}{[(k+q)^2+m^2](k^2+m^2)}. \tag{C.7}$$

This momentum integral can be easily carried out by standard quantum field theory textbook procedures. We begin by simplifying the denominator through the introduction of a Feynman parameter:

$$\frac{1}{[(k+q)^2+m^2][k^2+m^2]} = \int_0^1 \frac{dx}{A^2}, \tag{C.8}$$

where the new term on the denominator is given by

$$A = x[(k+q)^2+m^2]+(1-x)(k^2+m^2) = k^2+2xk\cdot q+xq^2+m^2. \tag{C.9}$$

By making the substitution $k = l - xq$, the expression for A can be brought to the form

$$A = l^2+\Delta \tag{C.10}$$

with a $\Delta = m^2+x(1-x)q^2$. Next, to simplify the numerator of (C.7), we are going to use the following integral identities

$$\int \frac{d^dl}{(2\pi)^d}\frac{l^\mu}{A^2} = 0 \qquad \text{and} \qquad \int \frac{d^dl}{(2\pi)^d}\frac{l^\mu l^\nu}{A^2} = \int \frac{d^dl}{(2\pi)^d}\frac{\frac{1}{d}\delta^{\mu\nu}l^2}{A^2}. \tag{C.11}$$

Both of them hold provided that A only depends on the magnitude of l^μ.[2] Then, it follows that the numerator can be written as

$$\begin{aligned} A &= 2\delta^{\mu\nu}[(k+q)^2+m^2] - (2k+q)^\mu(2k+q)^\nu \\ &\xrightarrow{k=l-xq} 2\delta^{\mu\nu}[l^2+(1-x)^2q^2+m^2] - 4l^\mu l^\nu - (1-2x)^2 q^\mu q^\nu \\ &= \tfrac{2}{3}\delta^{\mu\nu}l^2 + 2\delta^{\mu\nu}(1-x)^2q^2 + 2\delta^{\mu\nu}m^2 - (1-2x)^2 q^\mu q^\nu. \end{aligned} \tag{C.12}$$

Returning to the expression for $\Pi^{\mu\nu}(q)$, we now have

$$\Pi^{\mu\nu}(q) = \frac{4}{g}\int_0^1 dx \int \frac{d^3l}{(2\pi)^3} \frac{\frac{2}{3}\delta^{\mu\nu}l^2 + 2\delta^{\mu\nu}(1-x)^2q^2 + 2\delta^{\mu\nu}m^2 - (1-2x)^2 q^\mu q^\nu}{(l^2+\Delta)^2}. \tag{C.13}$$

Since we are already working in imaginary time, the above integral on l^μ can be readily solved by means of the formulas

$$\int \frac{d^dl}{(2\pi)^d}\frac{1}{(l^2+\Delta)^n} = \frac{1}{(4\pi)^{d/2}}\frac{\Gamma(n-\frac{d}{2})}{\Gamma(n)}\Delta^{\frac{d}{2}-n} \tag{C.14}$$

and

$$\int \frac{d^dl}{(2\pi)^d}\frac{l^2}{(l^2+\Delta)^n} = \frac{d/2}{(4\pi)^{d/2}}\frac{\Gamma(n-\frac{d}{2}-1)}{\Gamma(n)}\Delta^{\frac{d}{2}+1-n}. \tag{C.15}$$

The result is

$$\Pi^{\mu\nu}(q) = \frac{g^{-1}}{2\pi^{3/2}}\int_0^1 dx \frac{\Gamma(\frac{1}{2})}{\Delta^{\frac{1}{2}}}\Big\{2\delta^{\mu\nu}\big[(1-x)^2 - x(1-x)\big]q^2 - (1-2x)^2 q^\mu q^\nu\Big\}. \tag{C.16}$$

However, as one should notice, the expression above is not manifestly gauge invariant. To unveil this feature we make the following substitution

$$(1-x)^2 \quad \to \quad \tfrac{1}{2}[(1-x)^2 + x^2] \tag{C.17}$$

which is valid within the integration domain $x \in [0,1]$. We are then able to arrive at

$$\Pi^{\mu\nu}(q) = \frac{1}{2\pi g}\int_0^1 dx \frac{(1-2x)^2}{\Delta^{\frac{1}{2}}}\big(q^2\delta^{\mu\nu} - q^\mu q^\nu\big) \equiv \big(q^2\delta^{\mu\nu} - q^\mu q^\nu\big)\Pi(q^2) \tag{C.18}$$

[2]The first formula follows from the symmetry of the integration limits. The second one is a direct consequence of Lorentz invariance.

with

$$\Pi(q^2) = \frac{1}{2\pi g} \int_0^1 dx \frac{(1-2x)^2}{\sqrt{m^2 + x(1-x)q^2}}. \tag{C.19}$$

So that it is now a trivial matter to verify that $\Pi^{\mu\nu}(q)$ indeed satisfies the Ward identity: $q_\mu \Pi^{\mu\nu}(q) = 0$.

Appendix D

The Minimal Coupling Origin in the Hopping Term

To justify the minimal coupling replacement performed in the main text, we just need to examine the effective hopping term H_t, since the minimal coupling of the time-like component $\mathcal{A}^0$ comes directly from its definition in (4.11). The hopping Hamiltonian is simply given by

$$H_t = \sum_{ij} \left(\tilde{t}_{ij} \bar{\eta}_i \eta_j e^{i\mathcal{A}_{ij}} + \text{h.c.} \right). \tag{D.1}$$

As we discussed, when embedded in an AF environment, H_t only couples sites belonging to the same Néel sublattice. So, to illustrate this procedure let us restrict our analysis to second nearest neighbor processes. This piece of H_t can be conveniently written as

$$H_{t'} = t' \sum_{\boldsymbol{x} \in A} \sum_{\boldsymbol{a}'} \Big(\bar{\eta}(\boldsymbol{x} + \boldsymbol{a}') \eta(\boldsymbol{x}) e^{i\mathcal{A}_{\boldsymbol{x}+\boldsymbol{a}',\boldsymbol{x}}} + \text{h.c.} \Big), \tag{D.2}$$

where $\boldsymbol{a}' = \{a(\hat{\boldsymbol{x}} + \hat{\boldsymbol{y}}), a(\hat{\boldsymbol{x}} - \hat{\boldsymbol{y}})\}$. Here, the opposite hopping processes are naturally mapped by the Hermitian conjugate. By taking the continuum limit $a \to 0$ in (4.44), we are led to $\mathcal{A}_{\boldsymbol{x}+\boldsymbol{a}',\boldsymbol{x}} \simeq \boldsymbol{a}' \cdot \boldsymbol{\mathcal{A}}$. Then, by assuming that the gauge field fluctuations are small, there will be no significative change in the topology of the FS, and one may go straightforwardly to the momentum space

$$H_{t'} = t' \sum_{\boldsymbol{k}} \sum_{\boldsymbol{a}'} \Big(\bar{\eta}_{\boldsymbol{k},A} \eta_{\boldsymbol{k},A} e^{-i\boldsymbol{a}' \cdot (\boldsymbol{k} - \boldsymbol{\mathcal{A}})} + \text{h.c.} \Big). \tag{D.3}$$

Hence, by substituing the explicit expressions for $\boldsymbol{a}'$, one will eventually find

$$H_{t'} = \sum_{\boldsymbol{k}} \Big[4t' \cos(k_x - \mathcal{A}_x) \cos(k_y - \mathcal{A}_y) \Big] \bar{\eta}_{\boldsymbol{k},A} \eta_{\boldsymbol{k},A}. \tag{D.4}$$

Finally, after expanding (D.4) around its band minima, one will get a free dispersion minimally coupled to the vector potential $\boldsymbol{\mathcal{A}}$.

Bibliography

[1] J. G. Bednorz and K. A. Müller, Zeitschrift für Physik B Condensed Matter **64**, 189 (1986).

[2] P. A. Lee, N. Nagaosa, and X. G. Wen, Rev. Mod. Phys. **78** (2006).

[3] A. Damascelli, Z. Hussain, and Z. X. Shen, Rev. Mod. Phys. **75**, 473 (2003).

[4] K. M. Shen *et al.*, Science **307**, 901 (2005).

[5] D. A. Wollman, D. J. Van Harlingen, W. C. Lee, D. M. Ginsberg, and A. J. Leggett, Phys. Rev. Lett. **71**, 2134 (1993).

[6] M. Platé *et al.*, Phys. Rev. Lett. **95**, 2 (2005).

[7] W. D. Wise *et al.*, Nature Physics **4**, 696 (2008).

[8] J. Chang *et al.*, Nature Physics **8**, 871 (2012).

[9] N. Doiron-Leyraud *et al.*, Nature **447**, 565 (2007).

[10] S. Badoux *et al.*, Nature **531**, 210 (2016).

[11] P. W. Anderson, Science **235**, 1196 (1987).

[12] R. Coldea *et al.*, Phys. Rev. Lett. **86**, 5377 (2001).

[13] A. Altland and B. D. Simons, *Condensed Matter Field Theory* (Cambridge University Press, 2010).

[14] E. Fradkin, *Field Theories of Condensed Matter Physics* (Cambridge University Press, 2013).

[15] E. C. Marino, *Quantum Field Theory Approach to Condensed Matter Physics* (Cambridge University Press, 2017).

[16] M. E. Peskin and D. V. Schroeder, *An Introduction To Quantum Field Theory* (Westview Press, 1995).

[17] A. M. Polyakov, *Gauge Fields and Strings* (CRC Press, 1987).

[18] T. C. Ribeiro and X.-G. Wen, Phys. Rev. Lett. **95**, 1 (2005).

[19] T. C. Ribeiro and X.-G. Wen, Phys. Rev. B **74**, 33 (2006).

[20] R. T. Pepino, A. Ferraz, and E. Kochetov, Phys. Rev. B **77**, 1 (2008).

[21] A. Ferraz, E. Kochetov, and B. Uchoa, Phys. Rev. Lett. **98**, 069701 (2007).

[22] P. Coleman, arXiv:1509.05769v1 (2015).

[23] N. D. Mathur *et al.*, Nature **394**, 39 (1998).

[24] T. Moriya and K. Ueda, Reports on Progress in Physics **66**, 1299 (2003).

[25] M. Oshikawa, Phys. Rev. Lett. **84**, 3370 (2000).

[26] A. Ferraz and E. A. Kochetov, Nuclear Physics B **853**, 710 (2011).

[27] K. Ohgushi, S. Murakami, and N. Nagaosa, Phys. Rev. B **62**, 6065 (2000).

[28] P. B. Wiegmann, Progress of Theoretical Physics Supplement **107**, 243 (1992).

[29] X. G. Wen, F. Wilczek, and A. Zee, Physical Review B **39**, 11413 (1989).

[30] P. A. Lee and N. Nagaosa, Phys. Rev. B **46**, 5621 (1992).

[31] M. Ogata and H. Shiba, Phys. Rev. B **41**, 2326 (1990).

[32] H. Shiba and M. Ogata, Int. J. Mod. Phys. B **05**, 31 (1991).

[33] F. D. M. Haldane, Phys. Rev. Lett. **50**, 1153 (1983).

[34] F. D. M. Haldane, Physics Letters A **93**, 464 (1983).

[35] P. A. Lee, Phys. Rev. Lett. **63**, 680 (1989).

[36] E. Dagotto, Rev. Mod. Phys. **66**, 763 (1994).

[37] I. Ivantsov, A. Ferraz, and E. Kochetov, Phys. Rev. B **96**, 195161 (2017).

[38] P. B. Wiegmann, Phys. Rev. Lett. **60**, 821 (1988).

[39] R. Shankar, Nuclear Physics B **330**, 433 (1990).

[40] A. E. B. Nielsen, G. Sierra, and J. I. Cirac, Nature Communications **4**, 2864 (2013).

[41] E. Kochetov and V. Yarunin, Phys. Rev. B **56**, 2703 (1997).

[42] S. Sachdev, arXiv:cond-mat/9303014 (1993).